NATIONAL ADVISORY COMMITTEE FOR AERONAUTICS

TECHNICAL NOTE 4204

COMPILATION OF INFORMATION ON THE TRANSONIC ATTACHMENT OF FLOWS AT THE LEADING EDGES OF AIRFOILS

By Walter F. Lindsey and Emma Jean Landrum

Langley Aeronautical Laboratory
Langley Field, Va.

Washington
February 1958

NATIONAL ADVISORY COMMITTEE FOR AERONAUTICS

TECHNICAL NOTE 4204

COMPILATION OF INFORMATION ON THE TRANSONIC ATTACHMENT OF FLOWS AT THE LEADING EDGES OF AIRFOILS

By Walter F. Lindsey and Emma Jean Landrum

SUMMARY

Schlieren photographs have been compiled of the two-dimensional flow at transonic speeds past 37 airfoils having variously shaped profiles, some of which are related and vary in thickness and camber. The data for these airfoils were analyzed to provide basic information on the flow changes involved and to determine factors affecting transonic-flow attachment, which is a transition from separated to unseparated flow at the leading edges of two-dimensional airfoils at fixed angles of attack as the subsonic Mach number is increased.

INTRODUCTION

A transition from separated to unseparated flow on two-dimensional airfoils at fixed angles of attack was observed in some previous tests (refs. 1 and 2) at subsonic speeds as the Mach number was increased, and this transition is referred to herein as the transonic-flow attachment. This phenomenon, or effects of it, has been observed in tests of wings at supersonic speeds (ref. 3) and in investigations of two-dimensional unsteady flow at transonic speeds (ref. 4). Additional, but uncorrelated, information has been obtained in various investigations such as reference 5. Also, the flow change was discussed briefly in reference 6.

Previous work has shown that not only do undesirable force and moment changes occur at transonic-flow attachment (refs. 1 and 5) but also the attachment can be accompanied by unsteady flows (ref. 4). A study of the factors affecting this flow change has, therefore, been undertaken.

A compilation was made of data on 37 related and miscellaneous shapes of two-dimensional airfoils tested at angles of attack from 0°

to 12° under comparable conditions. These data were analyzed to provide a better understanding of the flow change involved in transonic-flow attachment and of the factors affecting the change.

SYMBOLS

C_p	pressure coefficient, $\frac{\text{(Local static pressure) - (Free-stream static pressure)}}{\text{(Free-stream dynamic pressure)}}$
c	chord of airfoil
c_{l_i}	design section lift coefficient (incompressible)
$c_{m,c/4}$	section pitching-moment coefficient measured about quarter-chord axis
c_n	section normal-force coefficient
M	free-stream Mach number uncorrected for jet-boundary effects
r	leading-edge radius
t	maximum thickness of airfoil
x	distance along chord
y_c	ordinate of camber line
α	angle of attack, deg
$\alpha - \arctan\left(\frac{dy_c}{dx}\right)_{0.075c}$	attitude of forebody

Subscripts:

att	condition for transonic-flow attachment
cr	critical, corresponding to $M_l = 1.0$
f	flow-field measurements from static-pressure orifices in tunnel wall at end of model
l	local, as on model surface

APPARATUS

Previous attempts to correlate data from various two-dimensional transonic facilities have indicated that numerical differences exist in an unsystematic manner because of various factors involved in the tests. These factors are Reynolds number, humidity, tunnel-boundary conditions, and testing techniques. As a consequence, it was considered desirable that the compilation be made from results obtained in facilities that were closely related even though they had different test-section configurations. The facilities at the Langley Laboratory from which data for two-dimensional models were available are shown in figure 1.

The Langley rectangular high-speed tunnel (ref. 1) was a two-dimensional closed-throat facility utilizing compressed air in an induction jet to induce atmospheric air to flow through the 4- by 18-inch test section. (See fig. 1(a).) The data from this facility were subject to moisture-condensation effects, to choking of the flow, and to jet-boundary corrections. The jet-boundary corrections produced a corrected Mach number higher than the indicated value. The Reynolds number in this tunnel at a Mach number of 0.8 for a 4-inch-chord model was approximately 1.2×10^6.

The closed-throat tunnel was revised into a two-dimensional open-throat version (fig. 1(b)) having a 4- by 19-inch test section. (See ref. 5.) This facility utilized the induction nozzle to induce air to flow through the test section but was housed within a room in order to alleviate the humidity or condensation problems to some extent. (See ref. 7.) The open boundaries above and below the model changed the magnitude and direction of the jet-boundary effects and eliminated the usual choking restriction. (See ref. 5.) The Mach number correction for jet-boundary effects for this facility was indicated in reference 5 to be small.

In order to eliminate the condensation problem, the tunnel shown in figure 1(b) was revised to operate on the blowdown principle from compressed dry air (dewpoint of -60° F) as shown in figure 1(c). (See ref. 7.) Although the stagnation pressure in this version could be varied from 15 to 32 lb/sq in. abs, the tests were usually conducted at a stagnation pressure of 20 lb/sq in. abs. The corresponding Reynolds number at a Mach number of 0.8 on a 4-inch-chord model was approximately 2×10^6.

The maximum Mach number limitation of 1.0 in the semiopen tunnel was overcome by constructing a transonic version with slotted walls above and below the model as shown in figures 1(d) and 1(e). The test section was 4 inches by 19 inches. This transonic facility, the Langley airfoil test

apparatus, could be operated at stagnation pressures from about 22 to 40 lb/sq in. abs. Tests were usually conducted on 4-inch-chord models at a stagnation pressure of 26 lb/sq in. abs and a Reynolds number of 2.8×10^6 at a Mach number of 0.8.

The comparison of data from the closed-throat tunnel (fig. 1(a)) with data from the revised facility (figs. 1(b) to 1(e)) is subject to error because of the difference in magnitude and direction of the jet-boundary corrections which, for an incompressible flow, are as follows:

Jet-boundary correction	Closed throat	Open throat
$M_{corrected}$	$1.012\ M_{test}$	$\approx M_{test}$
$\alpha_{corrected}$	$\alpha_{test} + 0.09c_n$	$\alpha_{test} - 1.85c_n$

The source of a more serious error is the effect of choking on the flow in the closed-throat tunnel. Because of the close proximity of the Mach numbers for flow attachment and for choking, some of the published data from tests in the closed-throat tunnel (fig. 1(a)) are not presented. Data presented herein are uncorrected and are in accordance with published results from these facilities because no reliable means of correcting the data exists. (See refs. 1 and 5.)

MODELS

The airfoil shapes included in this compilation of data are presented in table I. The shapes include symmetrical-wedge and circular-arc profiles, flat plates with rounded leading edges (ref. 8), NACA 16-series airfoils (ref. 9), NACA 6-series airfoils (ref. 10), 6-digit-series airfoils (ref. 11), and high-lift airfoils (ref. 12). Additional information on the leading-edge radius and the facility in which the airfoils having rounded leading edges were tested is presented in table II. The chord length of each model was 4 inches except for the 13-W-6.6 and 20-W-10 models (table I). These models were made by cutting off portions of the 10-W-5 model.

RESULTS AND DISCUSSION

General Description of Flow Change

Figure 2, which is from reference 1, shows the flow past a double-wedge airfoil (referred to as 1S-(70)(03)-(70)(03) in ref. 1 and as 6-W-7 herein) at various subsonic Mach numbers in the test facility shown in figure 1(a). Transition is observed from separated flow at Mach numbers below 0.75 to unseparated flow at Mach numbers of 0.77 and higher. The flow change that occurs at a Mach number of approximately 0.76 is called herein the transonic-flow attachment. This flow attachment was first observed in the facility shown in figure 1(a) at high subsonic Mach numbers on airfoils having sharp leading edges or on the supersonic type of airfoils (ref. 1) as shown in figures 2 and 3. Figure 4 (from ref. 1) shows that transonic-flow attachment also occurs on airfoils having rounded leading edges.

Effect of Flow Change on Forces

Force data on airfoils show a variation in the effects of the leading-edge transonic-flow attachment on the aerodynamic characteristics. (See refs. 1, 5, and 8.) The variations in effects extend from no change to a significant change (ref. 1). In all cases the direction of the change is the same for increasing Mach number at a constant angle of attack. The definite effects on lift are either a sudden large increase or the beginning of rapid increases in lift coefficient, independent of the location of the terminal shock (shock terminating the local supersonic-flow region) at flow attachment. For the moment coefficients, an abrupt increase in the positive direction occurs. The magnitude of the abrupt increase following flow attachment is naturally dependent on the location of the terminal shock. Data for a round-edged flat plate, taken from reference 8 and shown in figure 5, illustrate that the magnitude of the positive break in pitching moment generally increases with angle of attack, and the Mach number at which the break occurs also increases with angle of attack. The lift-coefficient data at high angles of attack show the previously mentioned characteristic of a rapid increase in lift at flow attachment. The occurrence and magnitude of these force changes accompanying strong overexpansion of the flow on the airfoil are considered undesirable.

Factors Affecting Flow Attachment

Explanation for flow attachment.- Several factors affect the flow around leading edges of airfoils, in general. In the low-speed range, an increase in Mach number produces increases in the adverse pressure

gradient and, consequently, contributes to flow separation. A major factor affecting flow transition is shown later to be the origin and expansion of a region of supersonic flow above the surface of the model with increase in free-stream Mach number. Since pressures are propagated at the velocity of sound, a region of supersonic flow imposes an obstruction to the forward propagation of pressures (ref. 13) and produces a large reduction in upwash approaching the leading edge (refs. 14 and 15). The reduction in upwash assists in eliminating flow separation from the leading edge. The growth of the supersonic region and the attainment of supersonic velocities in close proximity to the leading edge (for example, fig. 6) establishes a condition that permits a supersonic type of expansion to occur "around the corner" formed by the leading edge. This flow behavior, in its most simple concept, is similar to a Prandtl-Meyer turn. If the factors that affect flow transition are of sufficient magnitude, the separation at the leading edge is eliminated. On airfoils having sharp leading edges, however, a small bubble of separation remains at the leading edge as shown in figure 7 and also in figure 8 which are from reference 2. The flow around the bubble, and in many cases the flow around the rounded leading edges of conventional airfoils, overexpands and is directed toward the surface of the model. An oblique shock is, therefore, required to redirect the flow along the surface of the model. The foremost oblique shock that terminates above the model and is observed in some of the photographs of figures 2 to 4 and figure 6 is attributed to moisture condensation. This shock is identified and designated "condensation" in figure 7. A transition in flow without benefit of upwash changes occurs with increase in Mach number at the abrupt bend in the surface of the double-wedge airfoil at the location of maximum thickness. (See fig. 9.)

General effects of airfoil shape.- The strength of the leading-edge flow phenomenon or of the transonic-flow attachment is used herein in order to define qualitatively one or more of the following flow characteristics involved in transonic-flow attachment: (1) severity or extent of leading-edge separation before attachment (figs. 2, 4, and 9) (2) extent or degree of overexpansion after attachment (fig. 6), (3) strength of the oblique shock resulting from overexpansion (figs. 4 and 9), and (4) size of the field affected by the phenomenon (fig. 9 and ref. 1).

The strength of the phenomenon, as indicated by the extent of separation at low speeds (fig. 9(a)) and by the size of the field affected after attachment (fig. 9(b)), is shown to weaken, and the phenomenon gradually fades out as the angle of attack is decreased. Figure 4 shows that the strength of the phenomenon, at a constant angle of attack of the airfoil, diminishes with increased bluntness of the leading edge of the airfoil. The decreased strength is shown by a decrease in overexpansion and oblique-shock strength at Mach numbers above attachment that are accompanied by a decrease in the severity or

extent of separated flow at low speeds. Similar effects of leading-edge bluntness are illustrated in figure 10 (test facility shown in fig. 1(b)) where an increase in bluntness is accomplished by increasing the ratio of thickness to chord. (The leading-edge radius is approximately proportional to the square of the thickness.)

Bluntness itself, however, is not the major controlling factor. In figure 11 the flows (in the facility shown in figure 1(b)) past three airfoils having the same leading-edge shape and thickness distribution but different amounts of camber show that, at a fixed angle of attack, both the leading-edge separation decreases with increase in camber and the strength of the flow attachment decreases with an increase in camber. (See ref. 8.) Figure 11 also shows that a decrease in angle of attack of a profile results in decreases in the strength of the phenomenon, as was shown in figure 9. Figure 11 substantiates the previous findings that a decrease in low-speed separation is accompanied by decreases in high-speed overexpansion.

Although the variety of flows shown in figure 11(a) is produced without changes in leading-edge bluntness, the flow changes are accompanied by decreases in the effective angles of attack of the leading edges. The large negative loads that occur on the leading edge of a highly cambered airfoil, as compared with the loads on an uncambered airfoil at the same nominal angle of attack, are evidence of the decreases in effective angle of attack. Further proof of the dependence of both low-speed separation and high-speed overexpansion upon the same aerodynamic feature is provided in figure 11(b). The effective angle of attack of the leading edge of the various cambered airfoils shown in figure 11(b) is roughly constant, and the leading-edge flow separation is approximately of the same extent on all three models at low speeds. The attending development and strength of the transonic-flow attachment for the models is also approximately the same.

These figures show that, for airfoil shapes conducive to extensive expansions of the flow around the leading edge, large overexpansions are produced at high speeds and subsequent large compressions are necessary.

Exception to generalized flow.- An exception to the flow generalities presented herein is shown in figure 12 where a flow condition at high speeds duplicates that which was observed for other airfoils after transonic-flow attachment. This flow condition in figure 12, however, occurs on the lower surface of a cambered airfoil (NACA 64A506) at a low angle of attack but at positive lift and without any low-speed separation from that surface. (See refs. 5 and 15.)

The modified transonic-flow attachment observed on the NACA 64A506 airfoil is produced by the principal contributing factor which is the development of a local region of supersonic flow previously mentioned. The

movement of the stagnation point around the leading edge in the direction of circulation (ref. 14) or the decrease in upwash that occurs on a lifting airfoil with increasing Mach number occurs here also. (See ref. 15.) In this case, however, the decreasing upwash is produced by the development of the supersonic region along the lower surface and is conducive to increasing the extent of the expansion of the flow around the leading edge onto the lower surface (ref. 15). The consequent progressively increasing aerodynamic angle of attack of the lower surface with increasing Mach number permits a smooth transition from unseparated flow at low speeds to an overexpanded flow at high speeds. The flow changes in figure 12 are directly comparable to those at the leading edge of an airfoil subjected to continuous increases in angle of attack at a constant, but high, subsonic Mach number as illustrated by figure 13. (See also fig. 9.)

The development of the supersonic region along the lower surface with increasing Mach number that produces additional increases in the expansion of the flow around the leading edge onto the lower surface must be accompanied by reductions in the extent of the expansions of the flow around the leading edge onto the upper surface. That these flow expansions exist is shown in figure 14 by the reduction in the strength of the oblique shock at the leading edge with increasing Mach number and by the shock development on the lower surface.

Effects of leading-edge shape of slab airfoils.- The effects of angle of attack on flow attachment for a blunt 2-percent-thick airfoil (from ref. 8) are shown by schlieren photographs and by corresponding pressure distributions in figure 15. These data substantiate the previous statement concerning the increase in strength of flow attachment with an increase in angle of attack from 4° to 8°.

An increase in the fineness ratio of the leading edge from 1:1 to 4:1 produces an alleviation of the overexpansion at an angle of attack of 8° for the attached flows (figs. 16 and 17). The pressure-distribution measurements for the slab profile with the 4:1 elliptical nose shape (fig. 16) indicate a gradual attachment, when compared with the abrupt attachment on the blunt profile (1:1). An increase in leading-edge fineness ratio to 10:1 caused the attachment to become even more gradual than was observed for the 4:1 leading edge. (See fig. 18.) A reduction in the angle of attack to 4° retained the relative effects of leading-edge shape but also eliminated separation and subsequent attachment on the sharpest leading edge (10:1) as indicated in figure 19.

These data (figs. 2 to 19, primarily from investigations reported in refs. 1, 5, and 8) indicate that, as the degree or extent of flow separation at low speeds decreases, the overexpansion at high speeds decreases and the Mach number for flow attachment decreases. The data also show that, as the angle of attack is decreased for any given profile,

the transonic-flow attachment gradually fades out at some low angle of attack, and the Mach number for flow attachment becomes indeterminate.

Summary of effects of airfoil configuration.- The effects of thickness, shape, and camber on Mach numbers for transonic-flow attachment are presented in figures 20 to 22. Data presented in figures 20 and 21 show the effect of angle of attack and thickness on the Mach number for flow attachment. The Mach number for attachment is used as a parameter since the presented data (figs. 2 to 19) show that strength or severity of attachment increases with Mach number. These data illustrate that, as the angle of attack is increased, the Mach number for flow attachment on the airfoil increases. Furthermore, at any given angle of attack, the Mach number for flow attachment decreases as the ratio of thickness to chord is increased.

Data given for cambered airfoils in figure 22 show that the general effects of camber and thickness are similar. The effect of camber, however, is related to the attitude of the forebody $\left[\alpha - \arctan\left(\frac{dy_c}{dx}\right)_{0.075c}\right]$ as shown in figure 22 and indicated by the discussion of figure 11.

Data on a symmetrical double-wedge profile with 0, 25, and 50 percent of the afterbody removed (obtained from the test facility of fig. 1(b) and given in fig. 23, and some data from ref. 16) indicated that the Mach number for attachment is dependent upon the forebody shape and that the afterbody of this elementary shape has no significant effect. Results from tests of sharp leading-edge airfoils (with various afterbody lengths and shapes from refs. 1, 16, and 17) presented in figures 20(d) and 21(b) show a decrease in the Mach number for flow attachment as the included angle of the leading edge increases, which is the same effect as that produced by increases in the ratio of thickness to chord (figs. 20(a) to 20(c)). Thus, an increase in the leading-edge angle can be considered to be equivalent to an increase in the ratio of thickness to chord.

The data on leading-edge fineness-ratio effects given in figure 21(d) show that an increase in the angle of attack of the slab airfoils is accompanied by an increase in the Mach number for flow attachment and, thus, the data are in agreement with the preceding results. The data, however, also show that an increase in the fineness ratio or sharpness of the leading edge produces a decrease in the Mach number for attachment. These results therefore appear to be in contradiction to the trend of the data from figures 2 to 12 and 21(a) to 21(c) which show the effects of thickness and of leading-edge angle. The apparent contradiction, however, is based on the assumption that there is a continuous linear variation of the effects of leading-edge shape throughout the range of leading-edge shapes covered by these data. The linearity or nonlinearity of

curves of the effects of leading-edge shape can be established by incompressible- and inviscid-flow theory.

Correlation based on leading-edge shape.- The leading-edge shape is, to a first approximation, dependent upon the leading-edge radius. Since the data have indicated that high-speed overexpansion and Mach number for flow attachment correlate with the extent of the flow separation at low speeds, a simple index for flow separation was examined as a function of the leading-edge radius for symmetrical airfoils expressed in terms of the thickness. The occurrence of flow separation is a function of the maximum negative pressure coefficient. The variation of the maximum negative pressure coefficients in incompressible flow at an angle of attack of 4° with leading-edge radius index are presented in figure 24(a). The nonlinear variation indicates that a moderately shaped nose, one that is neither blunt nor sharp, produces the lowest values of maximum negative pressure coefficient. The moderately shaped nose, therefore, is less likely to encounter flow separation.

The Mach numbers for flow attachment for airfoils at an angle of attack of 4° are presented as a function of leading-edge-radius index in figure 24(b). (Data of fig. 24(b) are from refs. 1, 5, and 18 and from fig. 20.) These data show a nonlinear variation in the Mach number for attachment with the leading-edge-radius index that is similar to the variation of the results for a theoretical pressure distribution. The data from various investigations on the effect of leading-edge shape on Mach number for flow attachment and on overexpansion are, therefore, in agreement and indicate that an airfoil having a moderately shaped leading edge will alleviate separation and reduce the adverse effects of transonic-flow attachment. Similar trends are shown by the data in figure 25 for angles of attack greater than 4°.

The Mach numbers for attachment for the NACA 2-006 airfoil $\left[\left(\frac{r}{t}\right)^{1/2} = 0.366\right]$ are very high in figure 25. This airfoil with its maximum thickness near the 13-percent-chord station (ref. 12) represents a marked departure in shape from the other airfoils represented in figure 25 and in table II. In addition, the leading-edge-radius index used (the abscissa) is too elementary to account for effects of marked changes in airfoil shape on the pressures and consequently on the Mach number for attachment. The index also does not fully account for the effects of change in the thickness-chord ratio between airfoils of different families, since in the analysis a trend was observed at an approximately constant index for the Mach number of attachment to decrease with increases in thickness-chord ratio and thereby to contribute to scatter in the data of figure 25.

Effect of testing techniques.- During the analysis, data for some models, such as the NACA 2-006 airfoil (fig. 25), were observed to deviate

considerably from the general trends; consequently, some tests originally made in the 4- by 19-inch semiopen tunnel (fig. 1(c)) were rerun in the airfoil test apparatus (fig. 1(d)). Comparisons of the Mach numbers for transonic-flow attachment obtained from the tests in the two different facilities showed agreement within ±0.02. (The accuracy in reading the Mach meter was ±0.01.)

Some of the data represent tests on a given model at different densities that correspond to a twofold change in Reynolds number from minimum values of 1.4×10^6 to 1.7×10^6. These results showed that the changes in Reynolds number had no effect. Tests on models with roughness strips extending from the 5- to 10-percent-chord stations also showed no effect of change in Reynolds number. The roughness formed by No. 180 carborundum grains increased the Mach number for attachment by about 0.03. Increasing the size of the roughness by using No. 60 carborundum grains produced an added increment in Mach number for attachment of about 0.03. These effects of roughness can be attributed to a simple spoiler action of the carborundum grains.

Comparison of Conditions for Attachment and for Shock-Induced Separation

The boundaries of angle of attack plotted against Mach number for transonic-flow attachment from figure 20(a) for NACA 64A-series airfoils of various thickness-chord ratios are shown in figure 26 together with the boundaries for shock-induced separation of the flow observed on these airfoils and obtained during the analysis for reference 19. These data and also the rough boundaries where the flow was observed in schlieren photographs to separate from the leading edge are presented in figure 27 in a more conventional manner of angle of attack plotted against Mach number. This presentation is an approximation of normal-force coefficient plotted against Mach number, as indicated by figure 28. Angle of attack is used as a parameter since its range for schlieren photographs exceeds that of the aerodynamic force data (ref. 5).

In figure 29 the aforementioned boundaries and some other pertinent data are presented separately for each airfoil of the four thicknesses. For all the airfoils, at a given angle of attack, transonic-flow attachment occurs with an increase in Mach number after leading-edge flow separation is established and is in accordance with previous discussions. For the 6-percent-thick airfoil an unsteady-flow boundary, obtained by using the methods of reference 4 on the data of reference 20, shows that unsteady flows occur under the conditions of simple leading-edge flow separation or shock-induced separation at $M = 0.8$, as would be expected from reference 4. The most important information provided by figure 29 is shown

for the NACA 64A004 airfoil at Mach numbers of approximately 0.75 and angles of attack between 4° to 6°. The data show that flow attachment occurs and is followed by an increase in Mach number before boundary-layer separation is produced by compression shocks. Similar behavior is shown by the data for the 6- to 9-percent-thick airfoils, although the transonic-flow attachment is weak. Data for an NACA 16-006 airfoil (fig. 30) also provide confirmation that shock-induced separation and leading-edge flow attachment are not necessarily related. At high angles of attack where the tendency for flow separation is great and the compression shocks are very strong, shock—boundary-layer interaction might have some effects. (See fig. 13.) Shock—boundary-layer interaction is stated to be a factor of possible influence on flow attachment in reference 21.

Types of Flow Attachment

An examination of many schlieren motion pictures of the flow past airfoils at constant angles of attack but with continuously changing Mach numbers showed variations in the flow behavior at attachment. The variations extended from an abrupt change (fig. 31) through a gradual attachment (fig. 17) to an oscillatory attachment (figs. 32 and 33). Successive frames in the strips of motion-picture film are presented in figures 31 to 34, and the computed change in Mach number between these successive frames is between 0.0001 and 0.0004. The abrupt attachment, as previously stated, brought about abrupt changes in normal force (fig. 5). The oscillatory attachment observed over a range of Mach numbers was generally followed by an interval in speed wherein the position of the shock and the separation point on the airfoil surface moved back and forth (fig. 22). The oscillatory attachment and the movement of the shock and separation point constitute unsteady flow conditions that are shown in reference 4 to contribute to buffeting.

A decrease in bluntness was observed in the photographs of flow for NACA 2-006 and 4-006 airfoils to cause an increase in the Mach number range of oscillatory attachment. Similar results were observed in the data for the NACA 0009-54 and 0009-64 airfoils as well as for the slab airfoils with leading edges of various fineness ratios. Data for the slab profiles (figs. 15 to 19) also showed that the increase in Mach number range for oscillatory attachment was accompanied by a softening or a change to a more gradual type of attachment. The change was a result of the small chordwise extent of supersonic flow and of the slow rearward movement of the terminal shock. The differences observed on the profiles with 4:1 and 10:1 leading edges were small. The slab profiles have leading-edge-shape indexes between approximately 0.7 and 0.2. (See table II.)

Although abrupt attachment occurred on the most blunt profile (leading-edge radius index of 0.7, fig. 15), it also occurred on the sharpest profile (leading-edge radius index 0, fig. 2). The change, therefore, from abrupt to oscillatory to gradual or weak attachment by either sharpening of blunt profiles or blunting of sharp profiles parallels the pattern of the strength of the phenomenon (figs. 24 and 25). The moderately shaped leading edge, consequently, appears to be beneficial, not only in minimizing both the probability of separation from the leading edge and strength of subsequent transonic-flow attachment, but also in relieving the abruptness of the change and the violence of the oscillations.

The data for the cambered airfoils (fig. 22) show that the Mach number range for oscillatory attachment increased with angle of attack for any given profile. The range also increased with increases in positive design lift coefficient. The practical aerodynamic situation is exaggerated in this comparison at fixed angles of attack. For a given lift coefficient and consequently lower angle of attack (ref. 5), cambered airfoils can encounter a more mild attachment than do the symmetrical or less-cambered airfoils. (See fig. 11 and ref. 20.) The increase in range at any given angle of attack is accompanied by a decrease of the Mach number at which the oscillations start. When the Mach number of attachment approaches 0.6, however, the attachment is either weak or of the gradual type ($\alpha = 8^\circ$ in fig. 22(a) and $\alpha = 10^\circ$ in fig. 22(b)).

These data (fig. 22) show that increases in the convexity of the surface for a given leading-edge shape have a strong influence on the increases for the Mach number range of oscillatory flow attachment. Data on symmetrical airfoils of the NACA 16-series having moderately shaped leading edges tend to confirm this result. The increase in thickness from 6 percent to 12 percent chord increased the surface convexity and tripled the range of oscillatory attachment. This behavior is similar to the movement of the shock and separation point along the surface of NACA 65A-series airfoils, as affected by the thickness. (See ref. 4.) Tests of two slab airfoils representing a threefold change in thickness-chord ratio but having the same leading-edge profile and surface curvature showed no effects of thickness on the oscillatory range.

Explanation of Oscillatory Attachment

When flow attachment starts, the air has a momentum component directed toward the surface of the model, as indicated by the overexpansion around the leading edge (fig. 32), and, momentarily, an unseparated flow can be established. The attachment produces a large increase in maximum local Mach number (figs. 6, 15, 16, and 18) that is accompanied by a corresponding increase in shock strength. The strong shock with the added influence of the surface curvature and the accompanying large back

pressure can cause the flow to separate, at least locally under the foot of the shock, and the influence can progress to the leading edge, possibly in an impulsive manner. The resulting separation causes the flow to revert to the initial condition of separated flow from the leading edge. With the influence of shock-induced separation spent and with the original conditions of reduced upwash and local supersonic flow still present, the cycle starts again with reattachment. The situation obviously represents an alternating unbalance between large pressure rises that exceed the large values required to separate a flow and small pressure rises that are too small to maintain a separated condition in the presence of a supersonic flow with its ability to flow around a corner. Interaction between shock and boundary layer is, thus, the major factor that contributes to the oscillatory nature of attachments.

Analysis of schlieren photographs and other data involving unsteady flows (for example, ref. 4) indicates that motion pictures at a rate of about 10,000 frames per second, with exposures of a few microseconds, would be needed to define completely the time history of 1 cycle of an oscillatory attachment. The available information, unfortunately, was limited to 300 frames per second. The photographs shown in figure 33, however, can provide information on the subject since the chordwise variations in the height of the separation boundary above the chord line can be considered indicative of the variations with time in the angular extent of separation (angle of mixing boundary with reference to the airfoil at any given chordwise distance).

The flow at the downstream edge of the photographs shown in figure 33 was at the leading edge of the airfoil about 4 milliseconds prior to the time of exposure. In frames designated A-3, B-2, B-4, C-2, C-4, D-2, D-4, (note blank at C-3) of figure 33 the height of the separation boundary indicates that a large angular extent of separation existed at the leading edge about 3 milliseconds prior to the exposure. The abrupt decrease in the height of the boundary upstream indicates that the angular extent of separation was eliminated in approximately 0.1 millisecond. A comparison of the height of the boundaries above the forward part of the model in these frames with the boundary heights for complete separation (for example, frames A-1, B-1, and C-1) indicated that both the chordwise and angular extent of separation increased somewhat more slowly to the initial state. The results shown in figure 33 tend to confirm the explanation of unsteady-flow attachment based on dynamic considerations.

The oscillatory attachment persists until the attitude of the airfoil or a component is changed, until the stream Mach number is increased so that either the back pressure or the shock strength is decreased, or until the shock is moved rearward on the airfoil to a position such that the accompanying separation cannot affect the flow at the leading edge. Flow-attachment oscillations then cease, but flow and shock oscillations on

the airfoil surface usually persist until additional changes occur in these same factors.

Photographs of the flow past a 9-percent-thick airfoil having a 30-percent-chord trailing-edge flap support the preceding deduction. At an angle of attack of 10° and at various flap deflections, oscillating attachment was observed as follows:

Flap deflection	Mach number range
+8° (down)	0.14
0°	.10
-5° (up)	.03

Figure 34 illustrates the flows observed for the flap deflection of 8°.

Flow Attachment in Three-Dimensional Flows

The preceding discussion of transonic-flow attachment has been confined to the flow past two-dimensional airfoils. In order to examine possible effects of aspect ratio, a study was made of the flow past a body of revolution because this body can be considered to represent a model of very low aspect ratio. The body used was a cylinder which had a length approximately equal to the diameter. The cylinder was supported at the 0° angle of attack with the axis of the cylinder parallel to the free stream. The two ends were cut off perpendicular to the axis, and the edge of the forward end was rounded. The flow past this model was examined with the model in a smooth condition and with roughness on the rounded edge. The flow photographs in figure 35 show that attachment occurred abruptly on this model. This same abruptness was also observed for blunt airfoils. A comparison of figure 35(a) with figure 35(b) shows that roughness caused the Mach number for attachment to increase. This effect is the same as that obtained on the airfoils, although the Mach number increment produced by roughness is larger for the body of revolution. The results, in general, indicate that transonic-flow attachment is not a phenomenon confined to two-dimensional airfoils but can be encountered in three-dimensional flow as well.

CONCLUDING REMARKS

Schlieren photographs have been compiled of the two-dimensional flow past 37 airfoils having variously shaped profiles, some of which are related and vary in thickness and camber. The data were analyzed to provide basic information on the flow changes involved in transonic-flow attachment, which is a transition from separated to unseparated flow at the leading edges of airfoils, and to determine factors affecting the flow change.

The analysis, which is in agreement with previous results, shows that the flow attachment occurs because local regions of supersonic flow on the upper surface decrease the upwash in front of the model and because the forward extension of these supersonic-flow regions along the airfoil to the vicinity of the leading edge permits a supersonic type of expansion to occur around the leading edge. The resulting expansion varies in extent from an expansion just sufficient to flow around moderately shaped leading edges to overexpansions requiring oblique shocks to redirect the flow along the surface of airfoils having blunt or sharp leading edges. The attachment occurs abruptly or in an oscillatory manner over a Mach number range when the leading edge is either too blunt or too sharp. The Mach number range for oscillatory attachment increases as the surface convexity of the airfoil is increased. Abrupt flow attachment can occur independently of shock—boundary-layer interaction. Shock—boundary-layer interaction, however, is the major factor that contributes to the oscillatory nature of attachments.

A study of the flow past a blunt-nosed body of revolution shows that the transonic-flow attachment occurs also in three-dimensional flows.

Langley Aeronautical Laboratory,
National Advisory Committee for Aeronautics,
Langley Field, Va., November 29, 1957.

REFERENCES

1. Lindsey, W. F., Daley, Bernard N., and Humphreys, Milton D.: The Flow and Force Characteristics of Supersonic Airfoils at High Subsonic Speeds. NACA TN 1211, 1947.

2. Stack, John: Shock Stalled Flows for Supersonic Type Airfoils at Transonic Speeds. Paper presented at 6th Int. Cong. Appl. Mech., (Paris), Sept. 22-29, 1946.

3. Brown, Clinton E., and Michael, William H., Jr.: On Slender Delta Wings With Leading-Edge Separation. NACA TN 3430, 1955.

4. Humphreys, Milton D.: Pressure Pulsations on Rigid Airfoils at Transonic Speeds. NACA RM L51I12, 1951.

5. Daley, Bernard N., and Dick, Richard S.: Effect of Thickness, Camber, and Thickness Distribution on Airfoil Characteristics at Mach Numbers Up to 1.0. NACA TN 3607, 1956. (Supersedes NACA RM L52G31a.)

6. Farren, William S.: The Aerodynamic Art. Jour. R.A.S., vol. 60, no. 547, July 1956, pp. 431-447.

7. Lindsey, Walter F., and Chew, William L.: The Development and Performance of Two Small Tunnels Capable of Intermittent Operation at Mach Numbers Between 0.4 and 4.0. NACA TN 2189, 1950.

8. Lindsey, Walter F., and Landrum, Emma Jean: Flow and Force Characteristics of 2-Percent-Thick Airfoils at Transonic Speeds. NACA RM L54I30, 1954.

9. Lindsey, W. F., Stevenson, D. B., and Daley, Bernard N.: Aerodynamic Characteristics of 24 NACA 16-Series Airfoils at Mach Numbers Between 0.3 and 0.8. NACA TN 1546, 1948.

10. Abbott, Ira H., von Doenhoff, Albert E., and Stivers, Louis S., Jr.: Summary of Airfoil Data. NACA Rep. 824, 1945. (Supersedes NACA WR L-560.)

11. Stack, John, and von Doenhoff, Albert E.: Tests of 16 Related Airfoils at High Speeds. NACA Rep. 492, 1934.

12. Loftin, Laurence K., Jr., and von Doenhoff, Albert E.: Exploratory Investigation at High and Low Subsonic Mach Numbers of Two Experimental 6-Percent-Thick Airfoil Sections Designed To Have High Maximum Lift Coefficients. NACA RM L51F06, 1951.

13. Lindsey, W. F.: Effect of Compressibility on the Pressures and Forces Acting on a Modified NACA 65,3-019 Airfoil Having a 0.20-Chord Flap. NACA WR L-76, 1946. (Formerly NACA ACR L5G31a.)

14. Stack, John, Lindsey, W. F., and Littell, Robert E.: The Compressibility Burble and the Effect of Compressibility on Pressures and Forces Acting on an Airfoil. NACA Rep. 646, 1938.

15. Lindsey, Walter F., and Dick, Richard S.: Two-Dimensional Chordwise Load Distributions at Transonic Speeds. NACA RM L51I07, 1952.

16. Humphreys, Milton D.: An Investigation of a Lifting 10-Percent-Thick Symmetrical Double-Wedge Airfoil at Mach Numbers Up to 1. NACA TN 3306, 1954.

17. Daley, Bernard N., and Lord, Douglas R.: Aerodynamic Characteristics of Several 6-Percent-Thick Airfoils at Angles of Attack From 0° to 20° at High Subsonic Speeds. NACA TN 3424, 1955. (Supersedes NACA RM L9E19.)

18. Humphreys, Milton D., and Robinson, Raymond A.: The Effect of Changes in the Leading-Edge Radius on the Aerodynamic Characteristics of a Symmetrical, 9-Percent-Thick Airfoil at High-Subsonic Mach Numbers. NACA RM L9L09, 1950.

19. Lindsey, Walter F., and Johnston, Patrick J.: Some Observations on Maximum Pressure Rise Across Shocks Without Boundary-Layer Separation on Airfoils at Transonic Speeds. NACA TN 3820, 1956.

20. Humphreys, Milton D., and Kent, John D.: The Effects of Camber and Leading-Edge-Flap Deflection on the Pressure Pulsations on Thin Rigid Airfoils at Transonic Speeds. NACA RM L52G22, 1952.

21. Wood, George P., and Gooderum, Paul B.: A Factor Affecting Transonic Leading-Edge Flow Separation. NACA TN 3804, 1956.

TABLE I.- MODELS

(a) Symmetrical NACA airfoils

16-004	16-006	16-009	16-012
		63A009	
64A004	64A006	64A009	64_1A012
65A004	65A006	65A009	
	66-006		
	0006-63	0009-44	
	2-006	0009-54	
	4-006	0009-64	

(b) Cambered NACA airfoils

64A206	64A506
16-206	16-506
16-212	16-512

(c) Miscellaneous shapes

Model notation	Profile	Leading-edge shape or included angle	Location of maximum thickness, percent chord
6-W-3	6-percent-thick symmetrical wedge	11.4°	30
6-W-7	6-percent-thick symmetrical wedge	4.9°	70
10-W-5	10-percent-thick symmetrical wedge	11.4°	50
13-W-6.6	10-percent-thick symmetrical wedge, trailing edge cut off	11.4°	66
20-W-10	20-percent-thick single wedge	11.4°	100
6-C-3	6-percent-thick symmetrical circular arc	23.3°	30
6-C-5	6-percent-thick symmetrical circular arc	13.8°	50
6-C-7	6-percent-thick symmetrical circular arc	9.8°	70
1:1	2-percent-thick flat plate or slab	1:1 ellipse	---
4:1	2-percent-thick flat plate or slab	4:1 ellipse	---
10:1	2-percent-thick flat plate or slab	10:1 ellipse	---
10:1	6-percent-thick flat plate or slab	10:1 ellipse	---

TABLE II.- LEADING-EDGE RADIUS INDEX AND TEST FACILITY

Airfoil	$\left(\frac{r}{t}\right)^{1/2}$	Tested in facility shown in figure -	Reference
16-004	0.140	1(d)	Unpublished
65A004	.158	1(b),(d)	4, Unpublished
64A004	.163	1(b)	5
16-006	.171	1(d)	Unpublished
16-206	.171	1(d)	Unpublished
16-506	.171	1(d)	Unpublished
66-006	.193	1(a)	1
65A006	.195	1(b),(d)	4, Unpublished
64A006	.202	1(b)	5, 20
64A206	.202	1(b)	5, 20
64A506	.202	1(b)	5, 20
16-009	.210	1(b),(d)	4, Unpublished
0009-44	.210	1(a),(b),(d)	18, Unpublished
10:1	.224	1(c)	8
65A009	.239	1(b),(d)	4, 5, Unpublished
16-012	.242	1(d)	Unpublished
16-212	.242	1(d)	Unpublished
16-512	.242	1(d)	Unpublished
64A009	.248	1(b)	5
0006-63	.258	1(a)	1, 17
63A009	.258	1(b)	5
0009-54	.260	1(a),(b),(d)	18, Unpublished
64_1A012	.288	1(b)	5
4-006	.304	1(c),(d)	Unpublished
0009-64	.315	1(a),(d)	18, Unpublished
4:1	.354	1(c)	8
2-006	.366	1(c),(d)	Unpublished
1:1	.707	1(c)	8

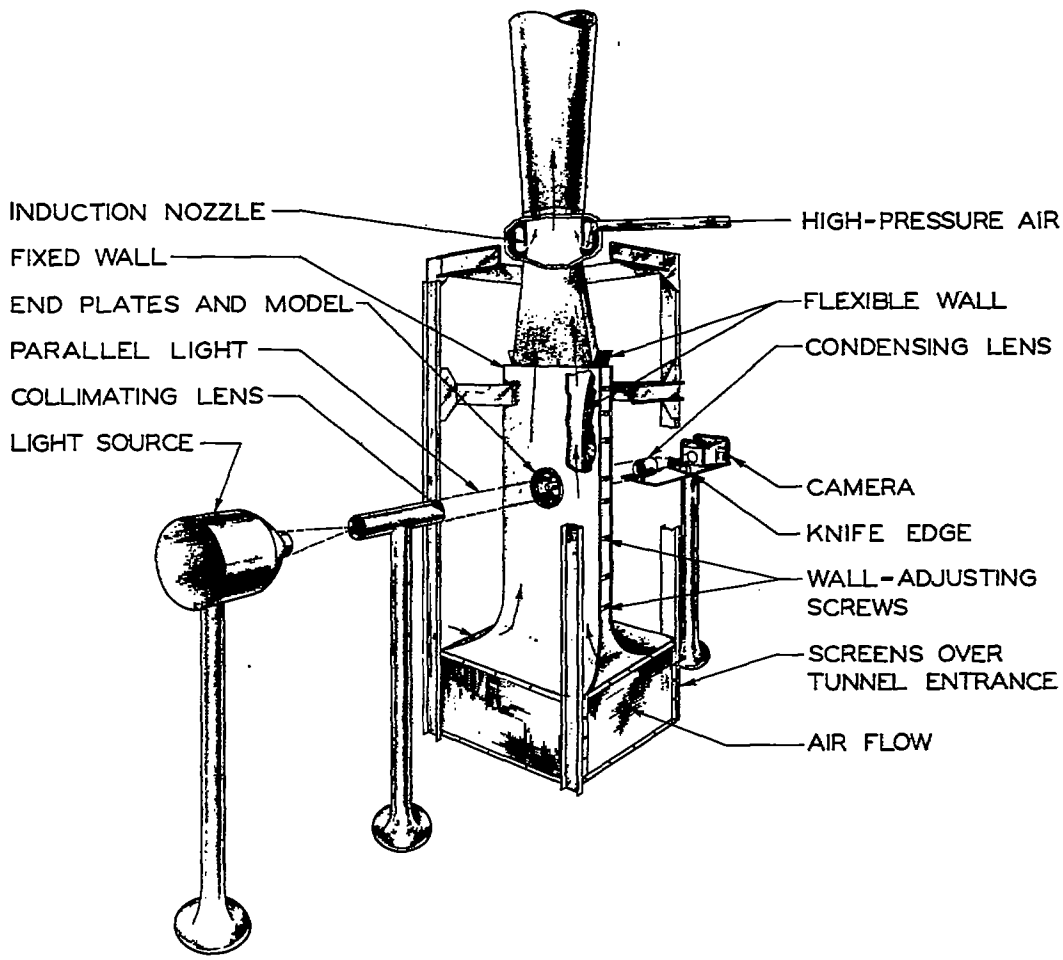

(a) Langley rectangular high-speed tunnel.

Figure 1.- Two-dimensional-flow test facilities.

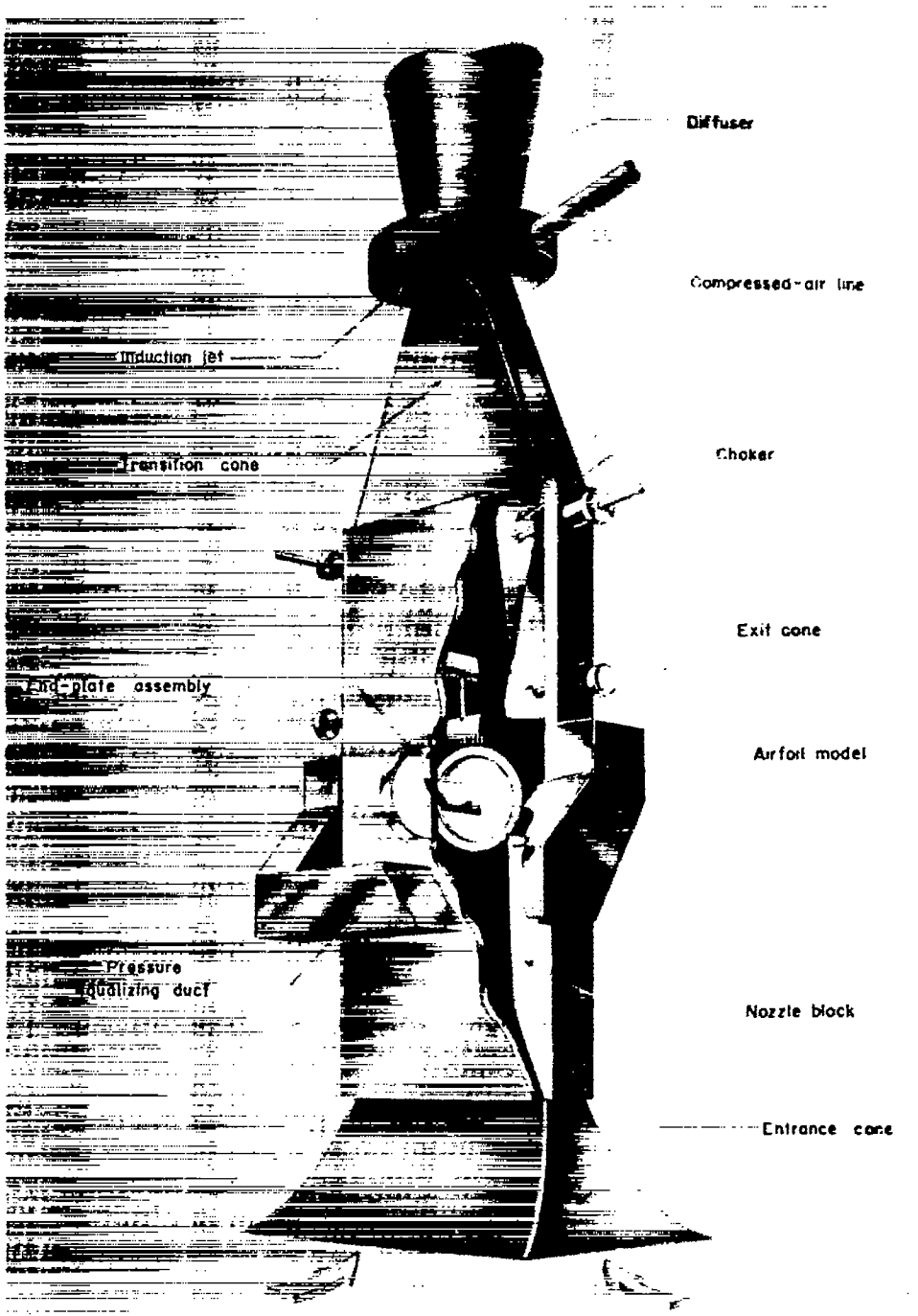

L-75177

(b) Langley 4- by 19-inch semiopen tunnel. Induction version.

Figure 1.- Continued.

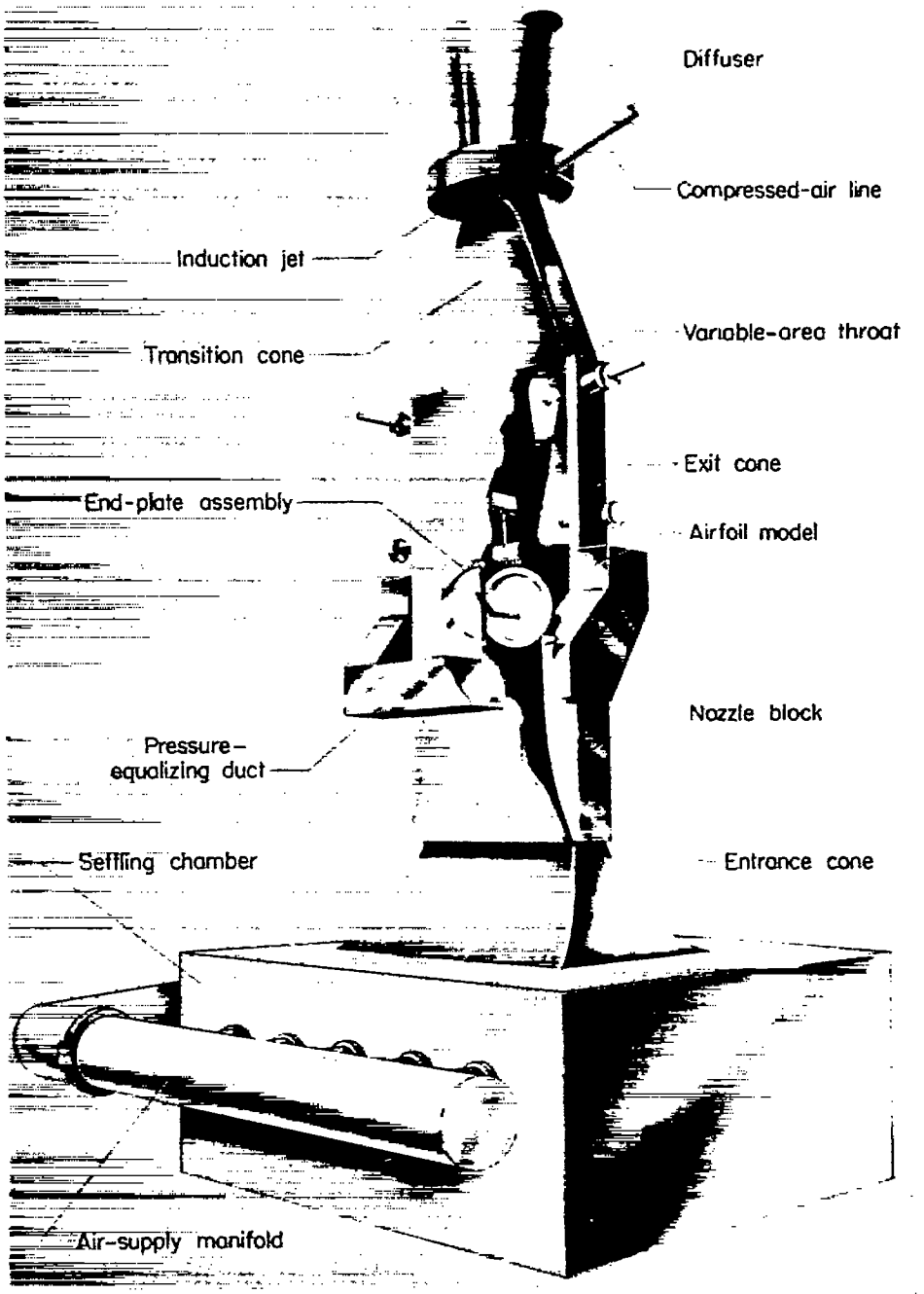

L-83293.1

(c) Langley 4- by 19-inch semiopen tunnel. Blowdown version.

Figure 1.- Continued.

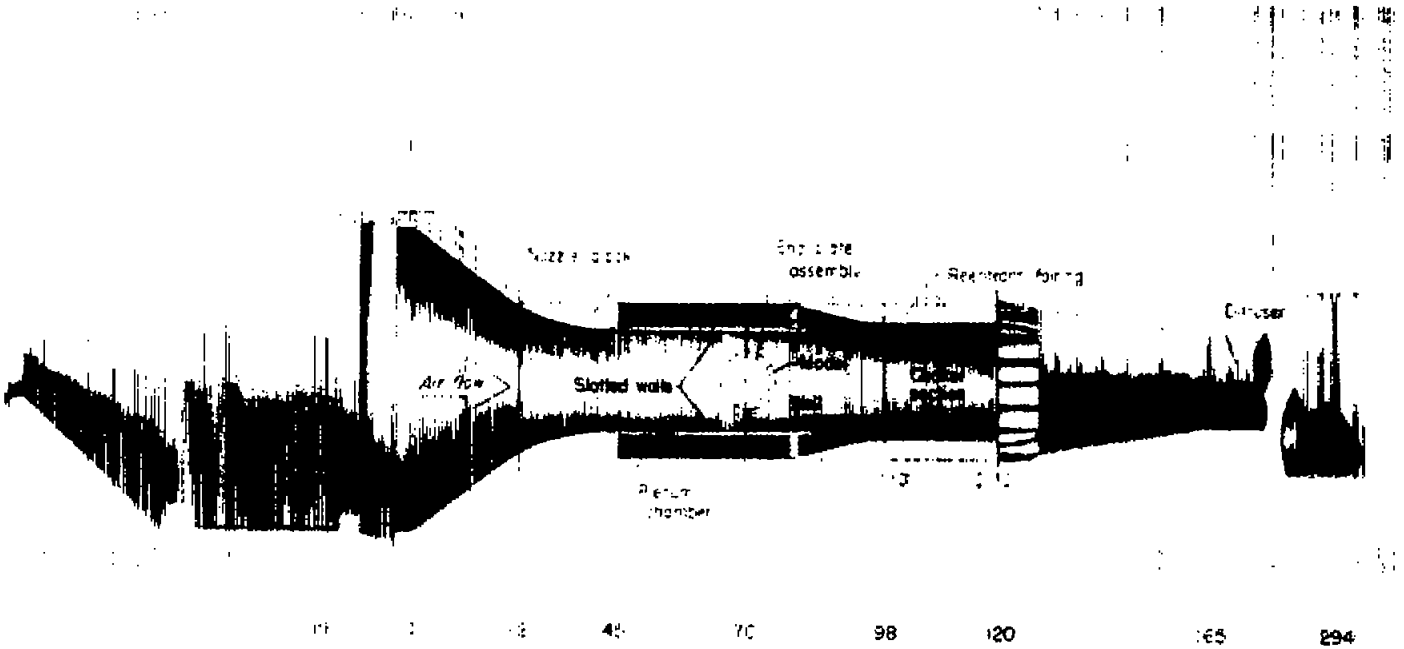

(d) Langley airfoil test apparatus. General view. L-57-599

Figure 1.- Continued.

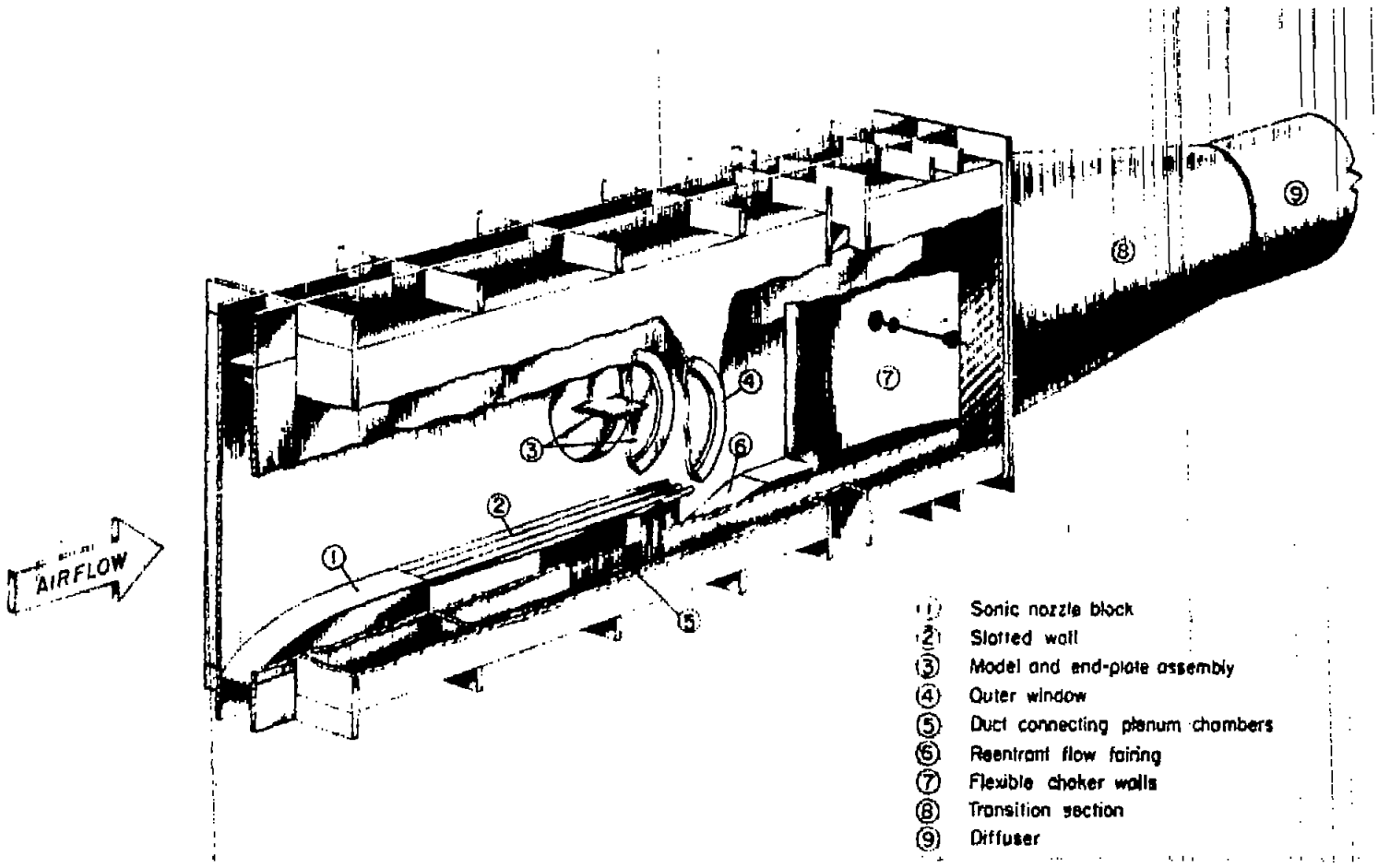

L-57-598

(e) Langley airfoil test apparatus. Test-section details.

Figure 1.- Concluded.

(a) M = 0.50.

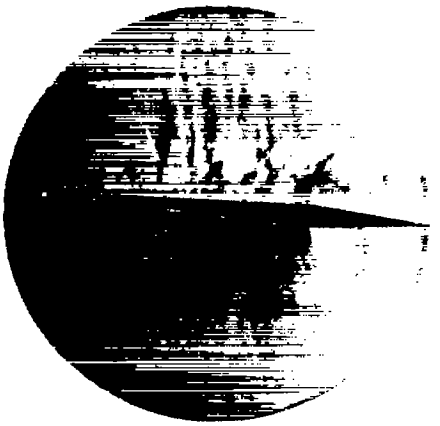

(b) M = 0.70.

(c) M = 0.72.

(d) M = 0.75.

(e) M = 0.77.

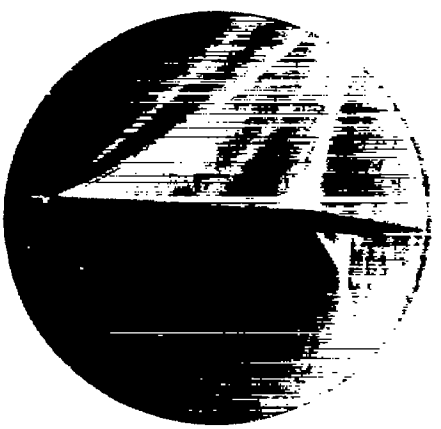

(f) M = 0.80.

L-57-2161

Figure 2.- Development of transonic-flow attachment on a 6-W-7 airfoil. $\alpha = 5.5^{\circ}$.

6-W-3

6-W-7

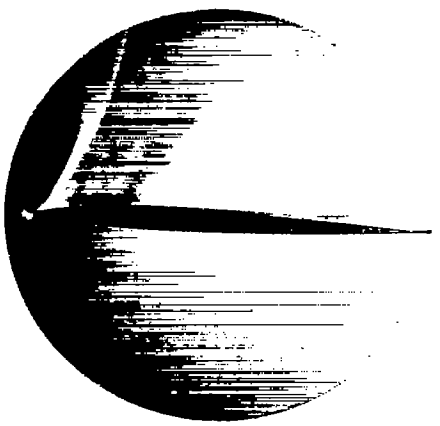

6-C-3

6-C-5

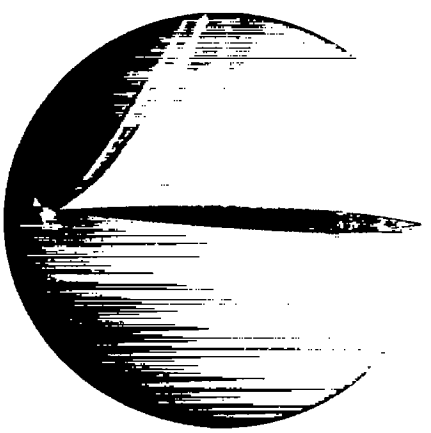

6-C-7

L-57-2162

Figure 3.- Flow attachment on various supersonic-type profiles. $\alpha = 4^{\circ}$; $M = 0.83$.

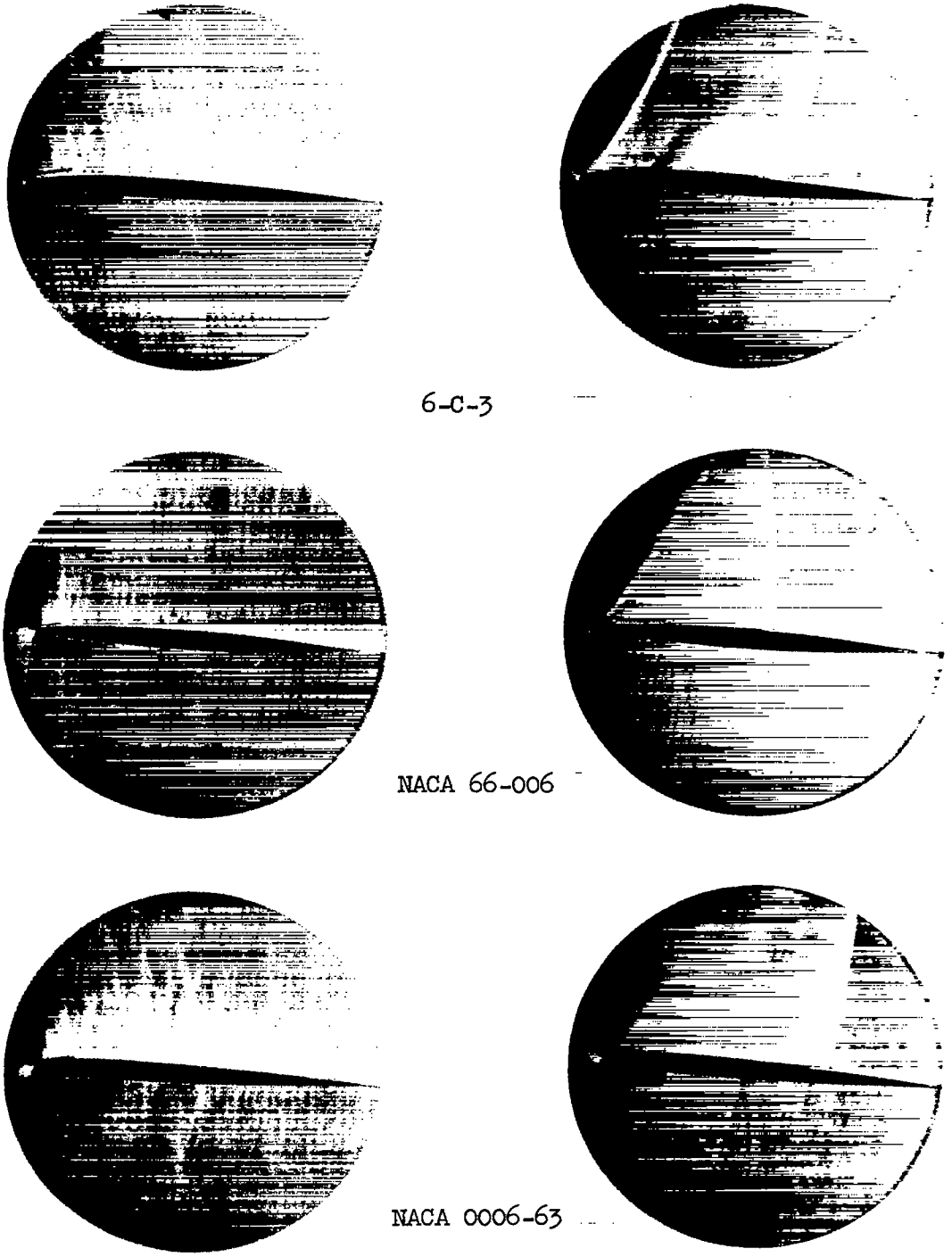

(a) M = 0.60. (b) M = 0.80.

L-57-2165

Figure 4.- Effect of leading-edge shape on flow. $\alpha = 4^{\circ}$.

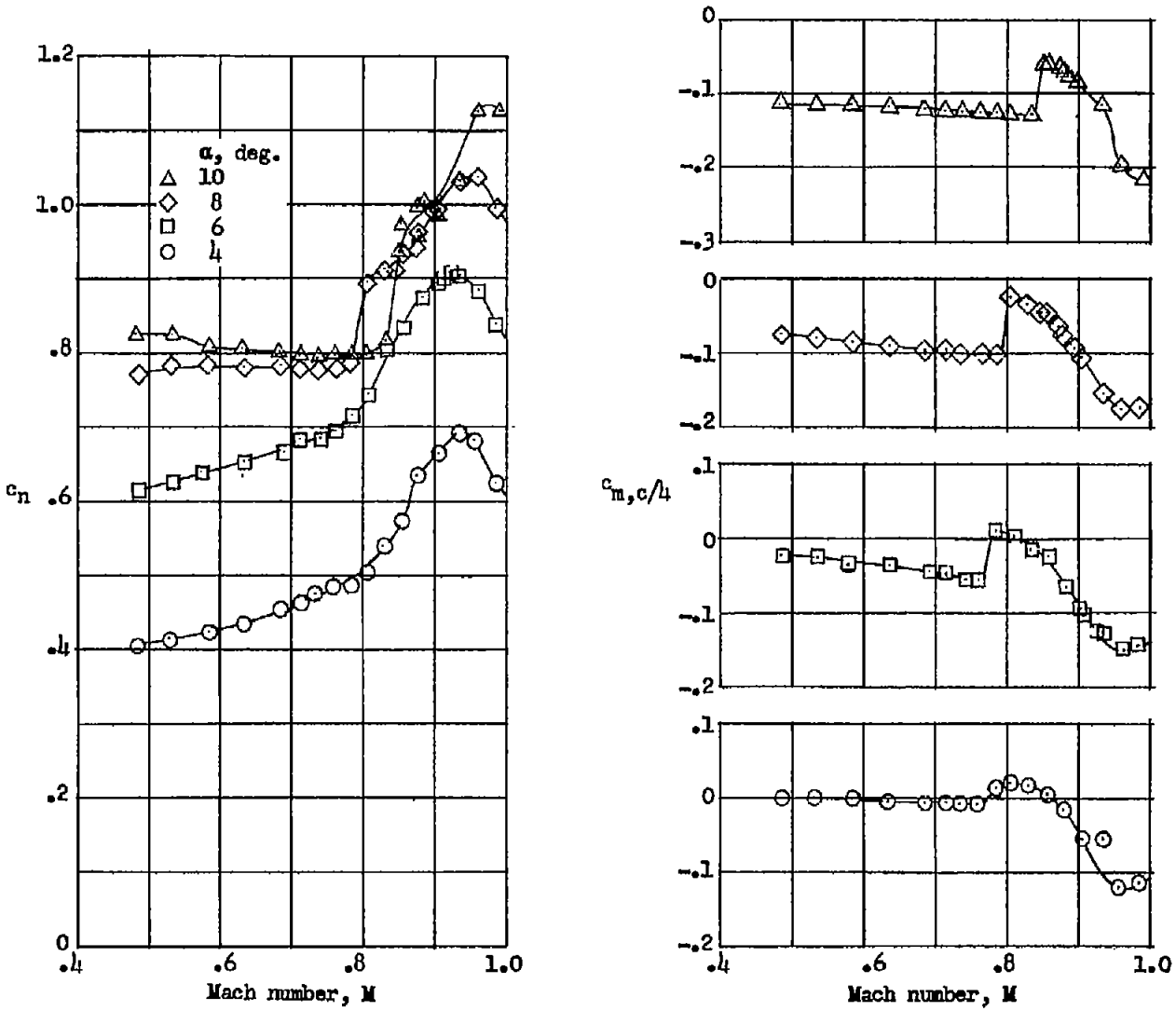

Figure 5.- Aerodynamic characteristics of a slab airfoil.

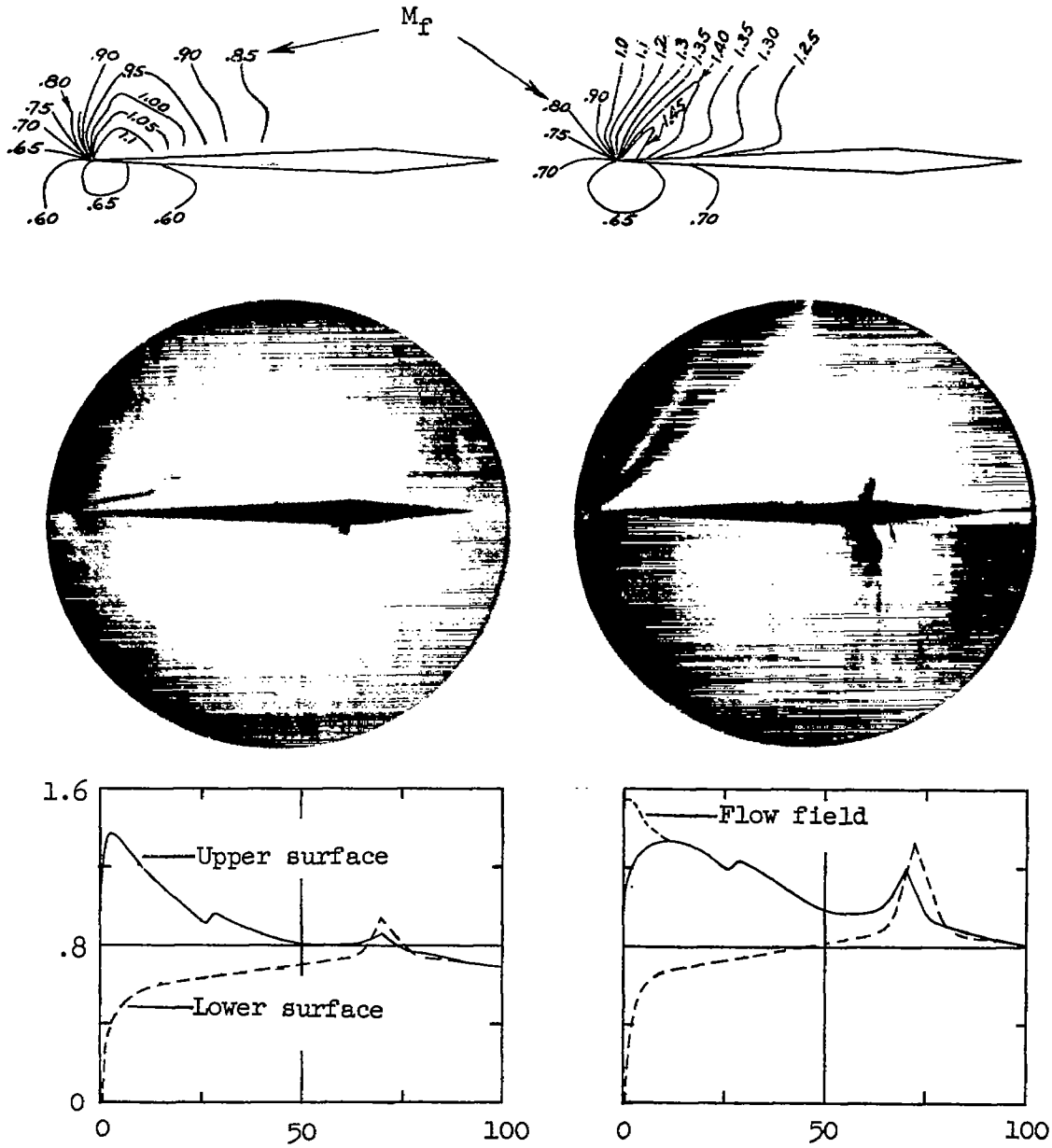

L-57-2163

Figure 6.- Details of flow before and after attachment. $\alpha = 4^\circ$.

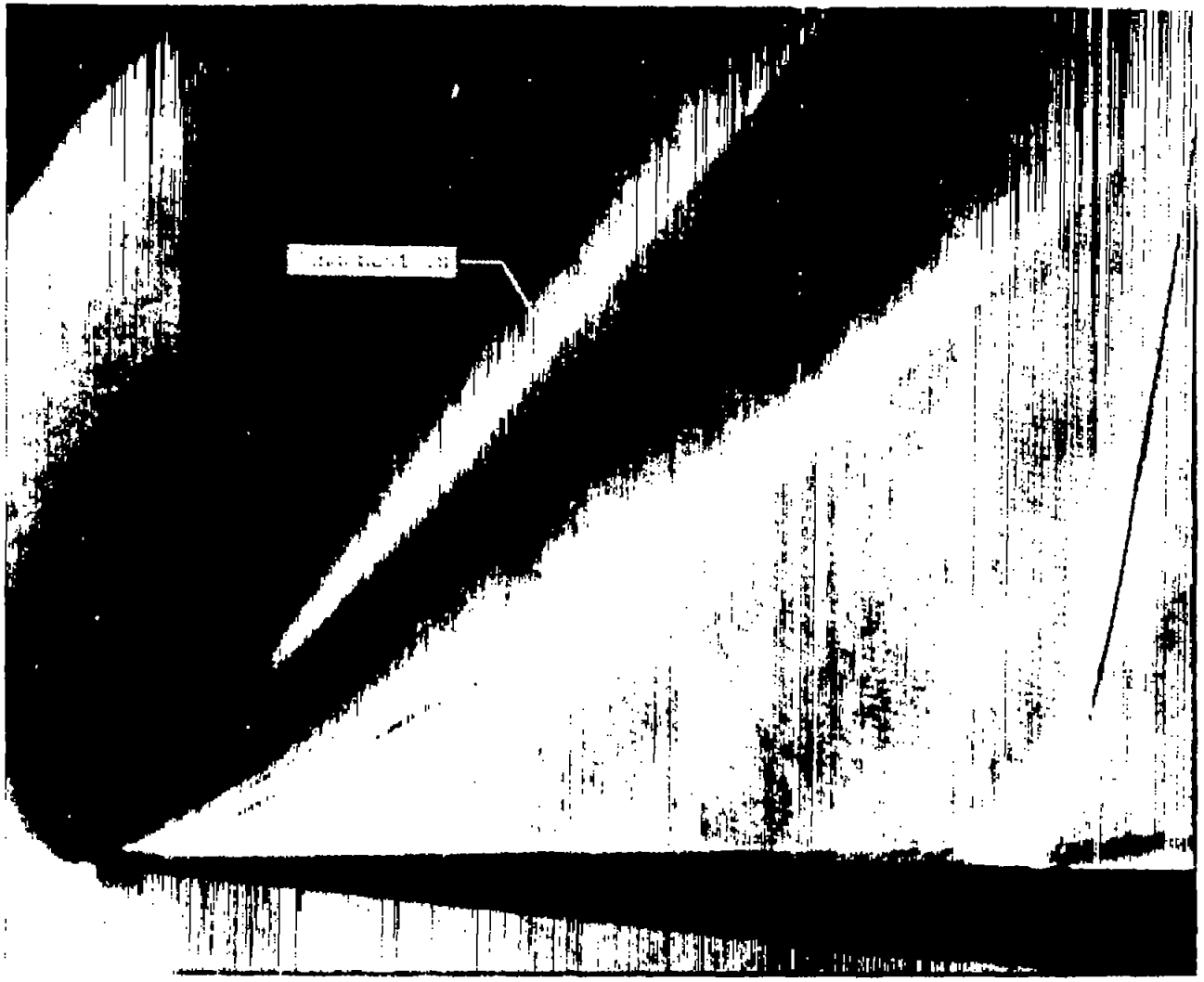

L-49753.1

Figure 7.- Photograph of flow near leading edge. Enlargement from figure 2(e).

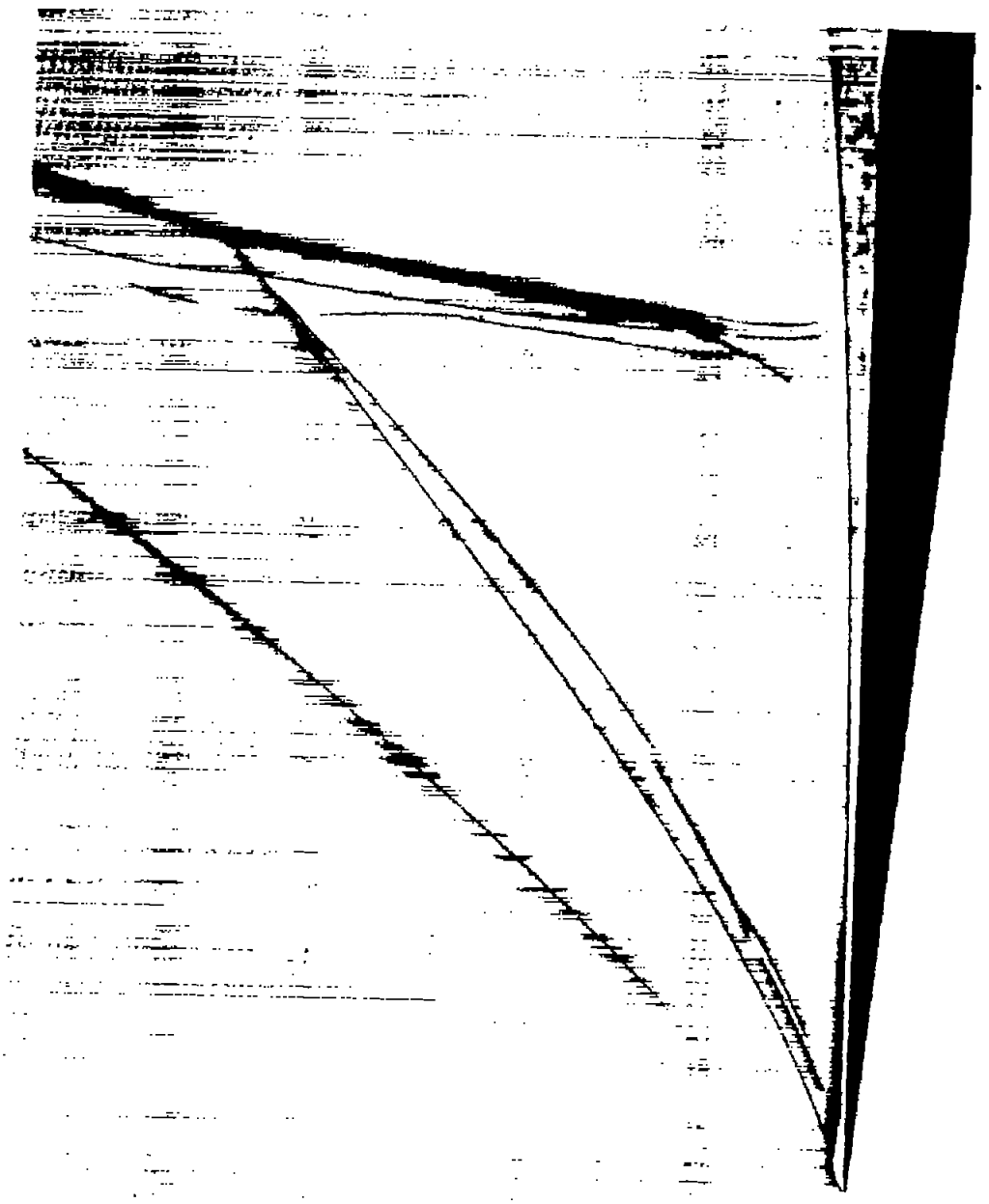

L-49754.1

Figure 8.- Schematic diagram of flow near leading edge. M = 0.769.

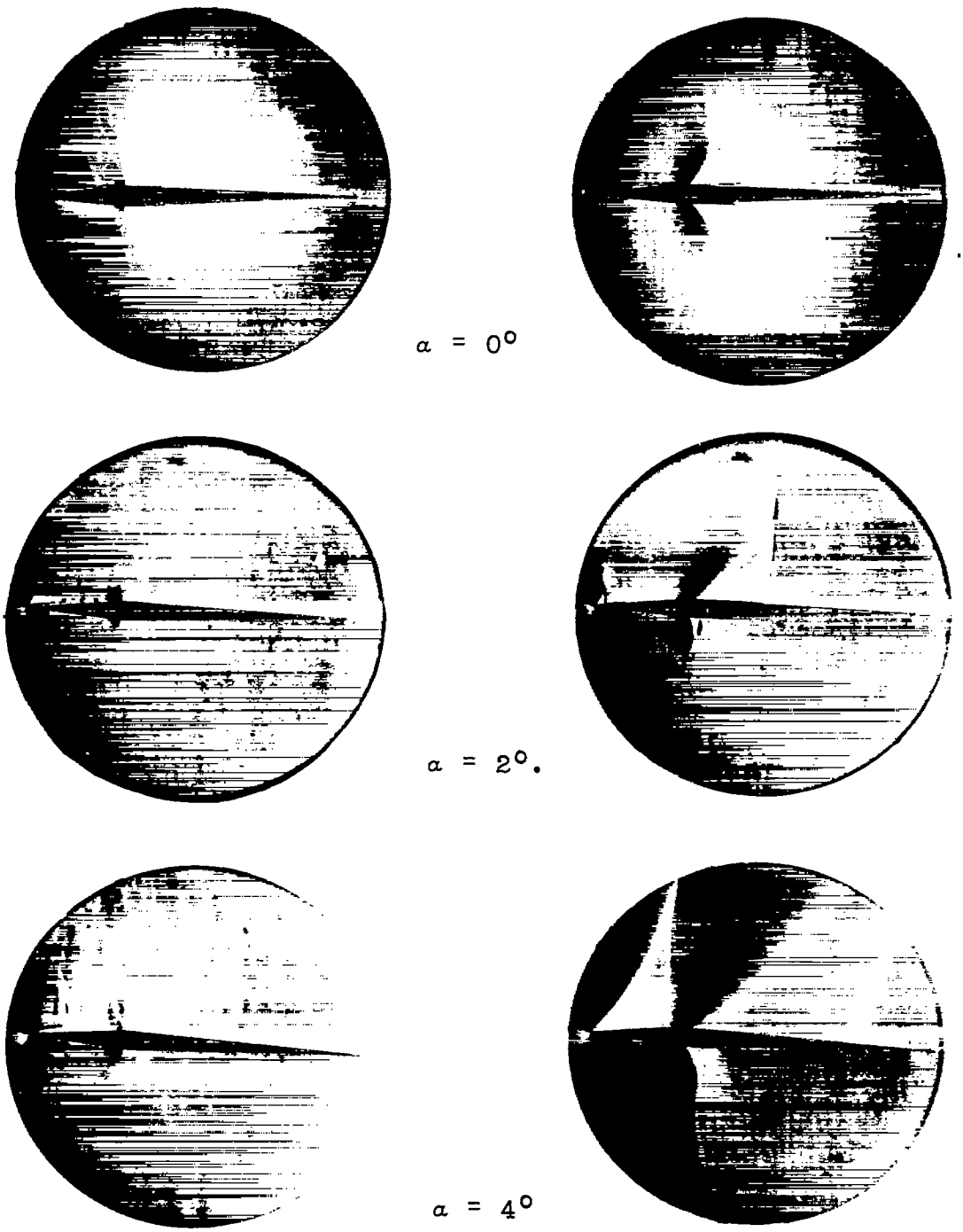

(a) M = 0.65. (b) M = 0.83.

L-57-2164

Figure 9.- Variation in flow attachment with angle of attack on a wedge airfoil (6-W-3).

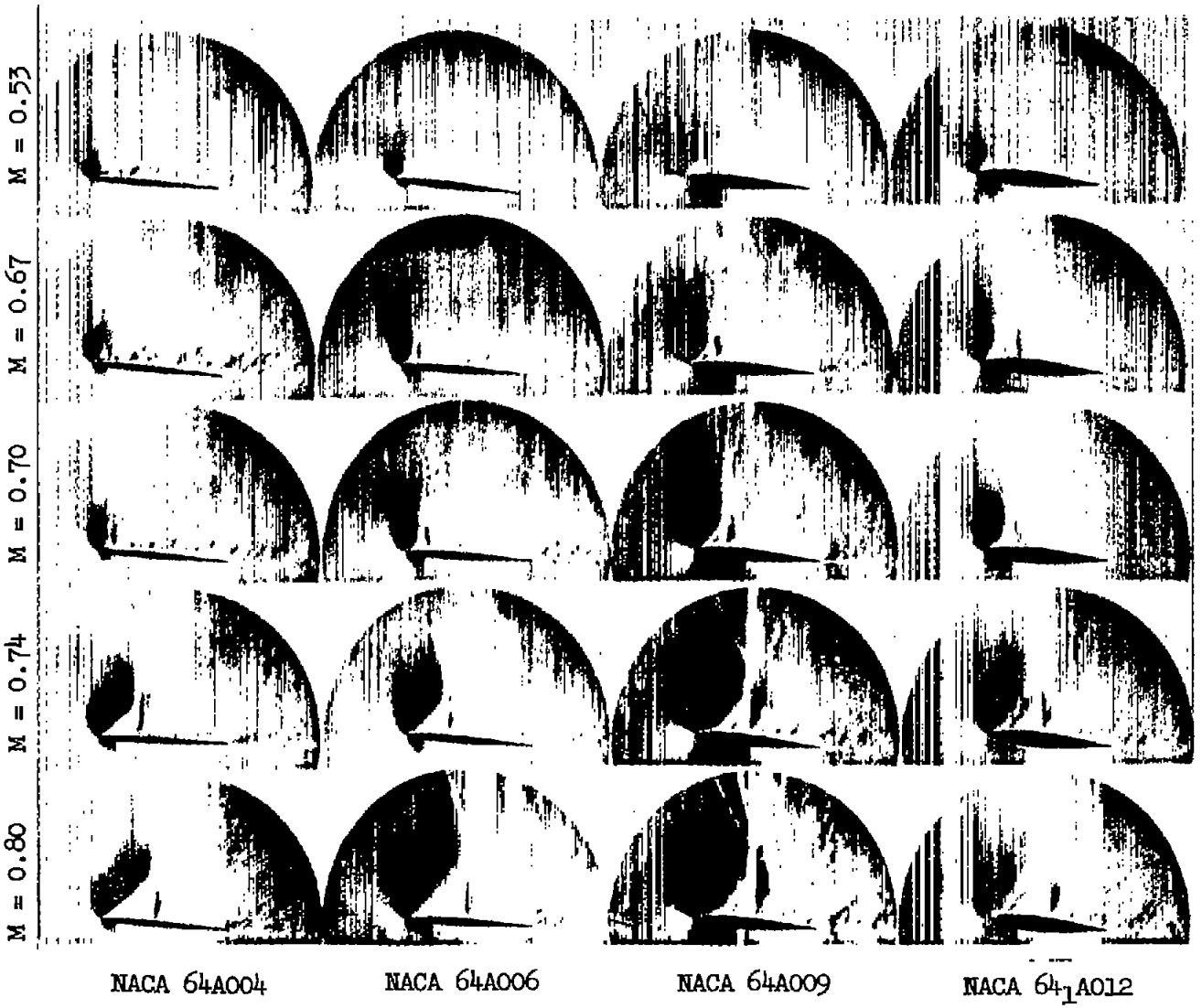

Figure 10.- Effects on flow of leading-edge bluntness due to changes in thickness. $\alpha = 6^{\circ}$.

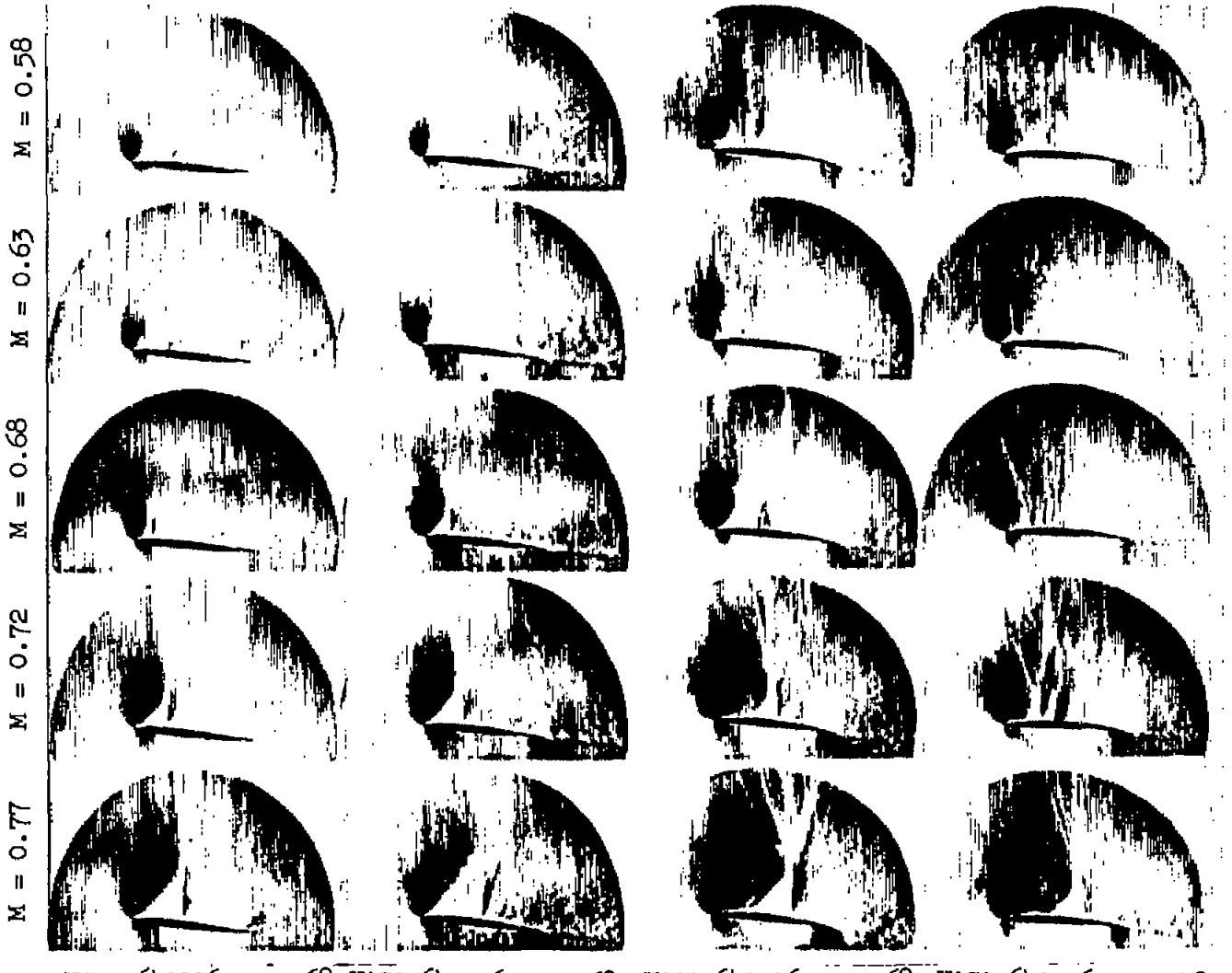

(a) Angle of attack or c_n approximately constant. L-86437

Figure 11.- Effects of camber.

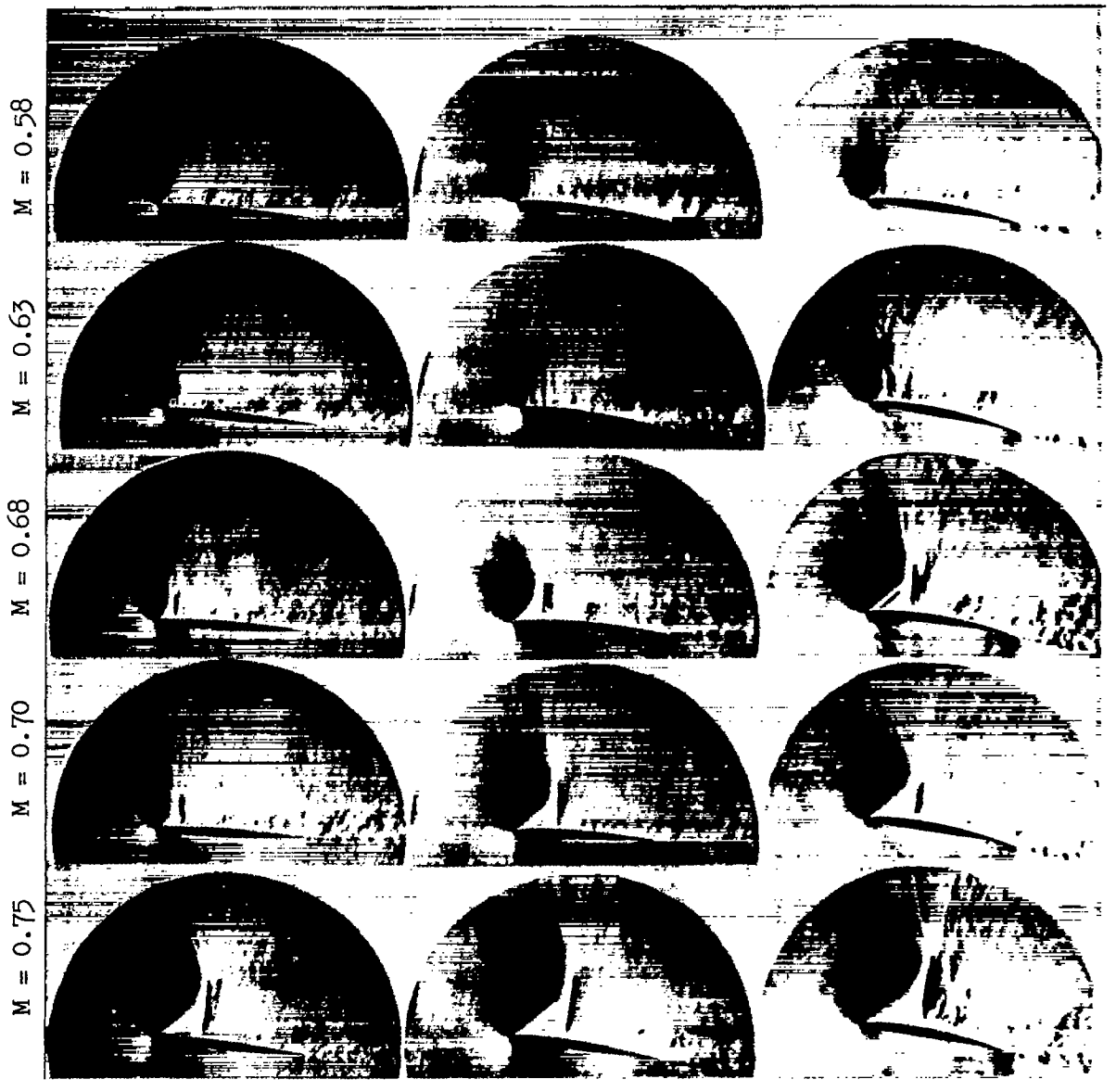

NACA 64A006; $\alpha = 6^\circ$. NACA 64A206; $\alpha = 8^\circ$. NACA 64A506; $\alpha = 10^\circ$.

(b) Low-speed separation approximately constant. L-86438

Figure 11.- Concluded.

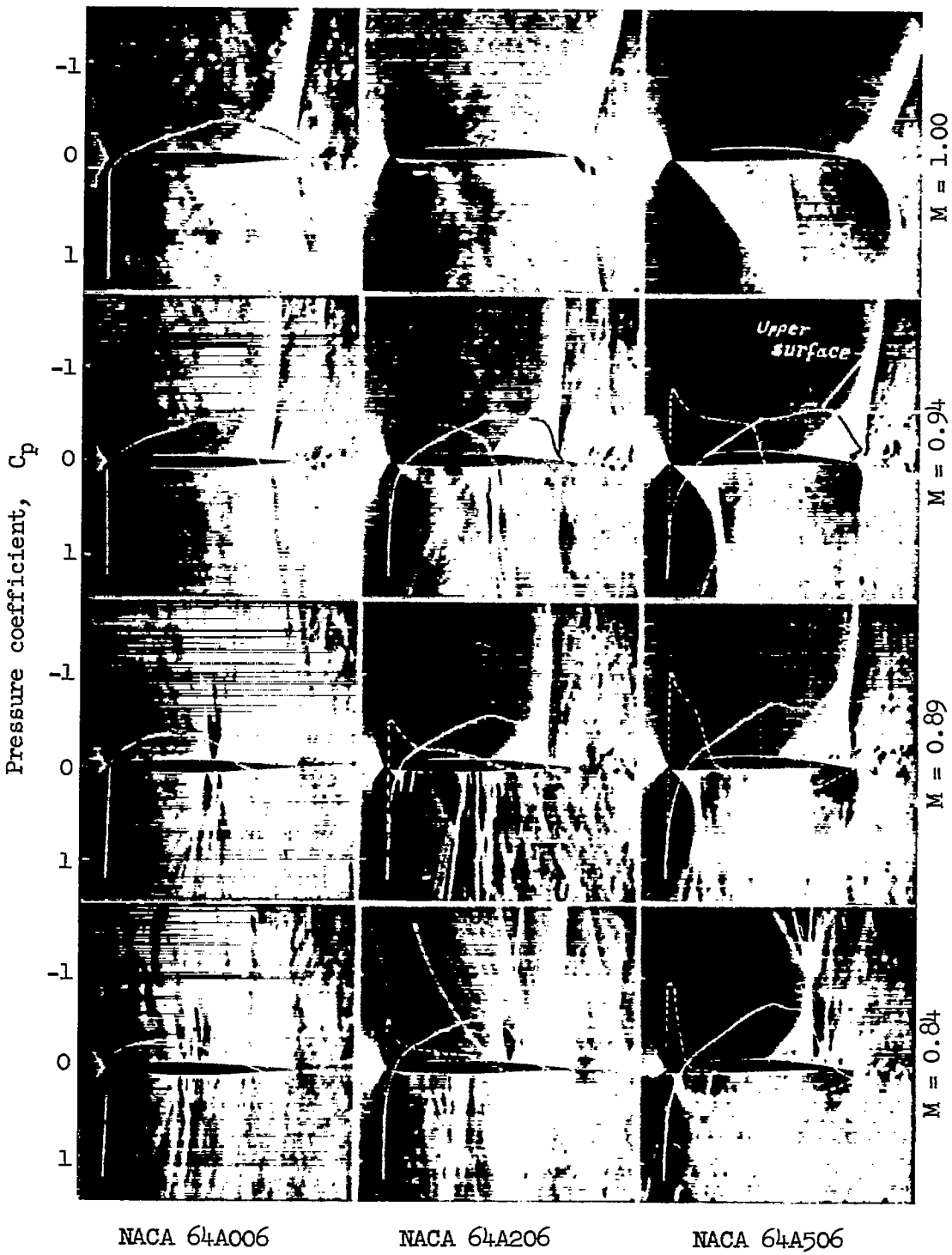

Figure 12.- Flow past cambered airfoils. $\alpha = 0^\circ$. L-73049.1

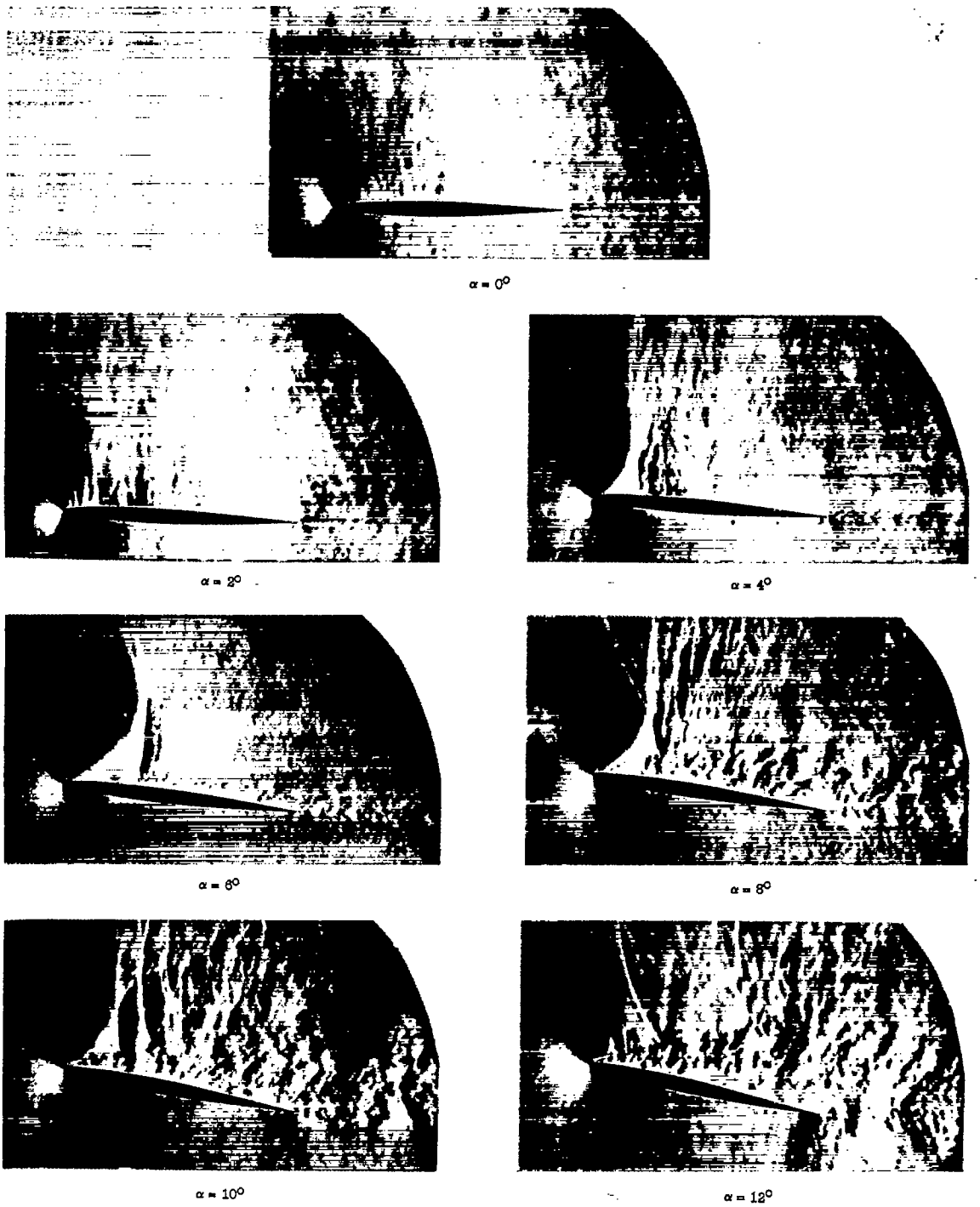

L-57-4404.1

Figure 13.- Change in leading-edge flow attachment with angle of attack. NACA 64A006 airfoil; M = 0.75.

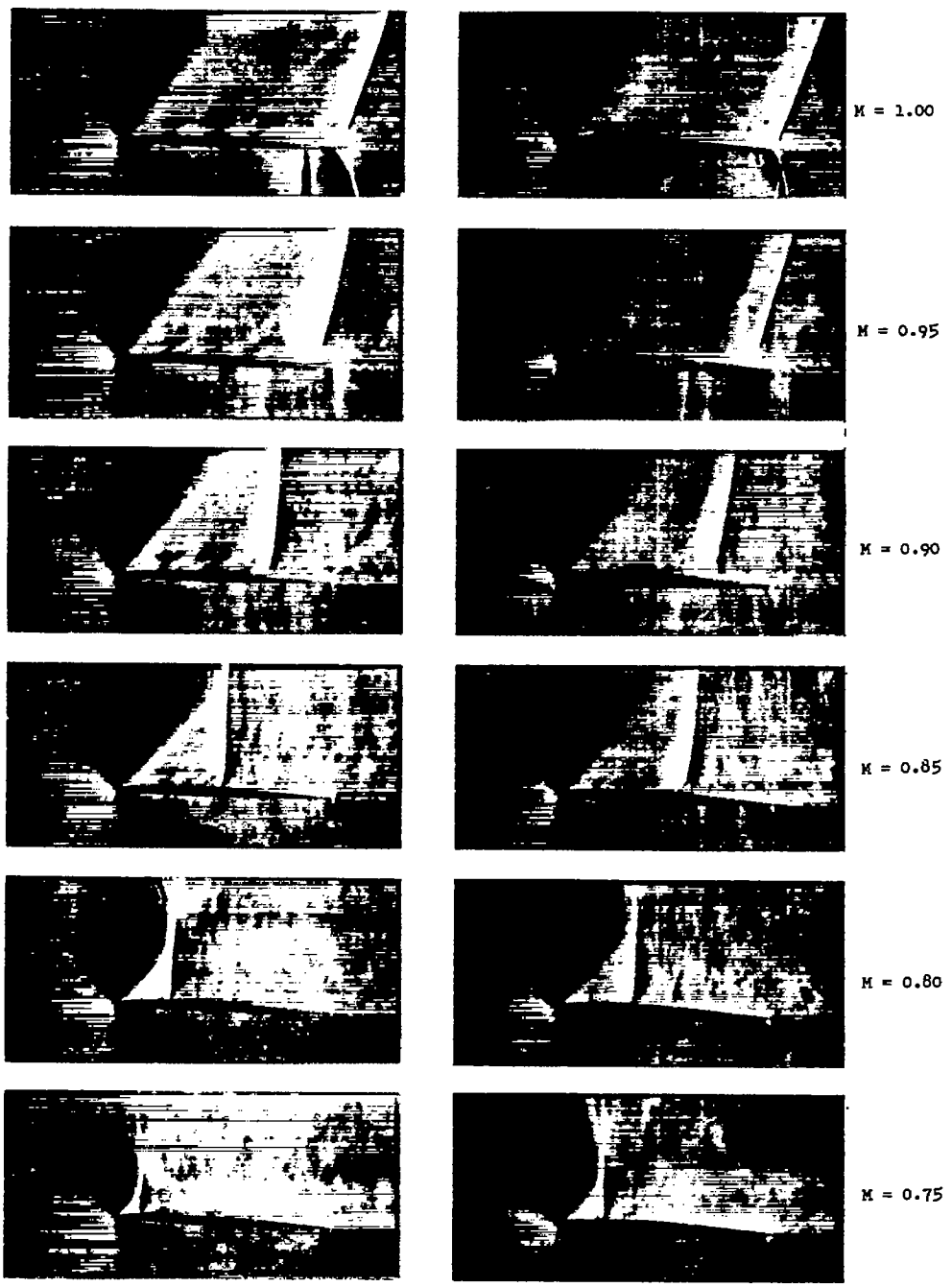

L-57-4403.1

Figure 14.- The decay in expansion around the leading edge at high Mach numbers.

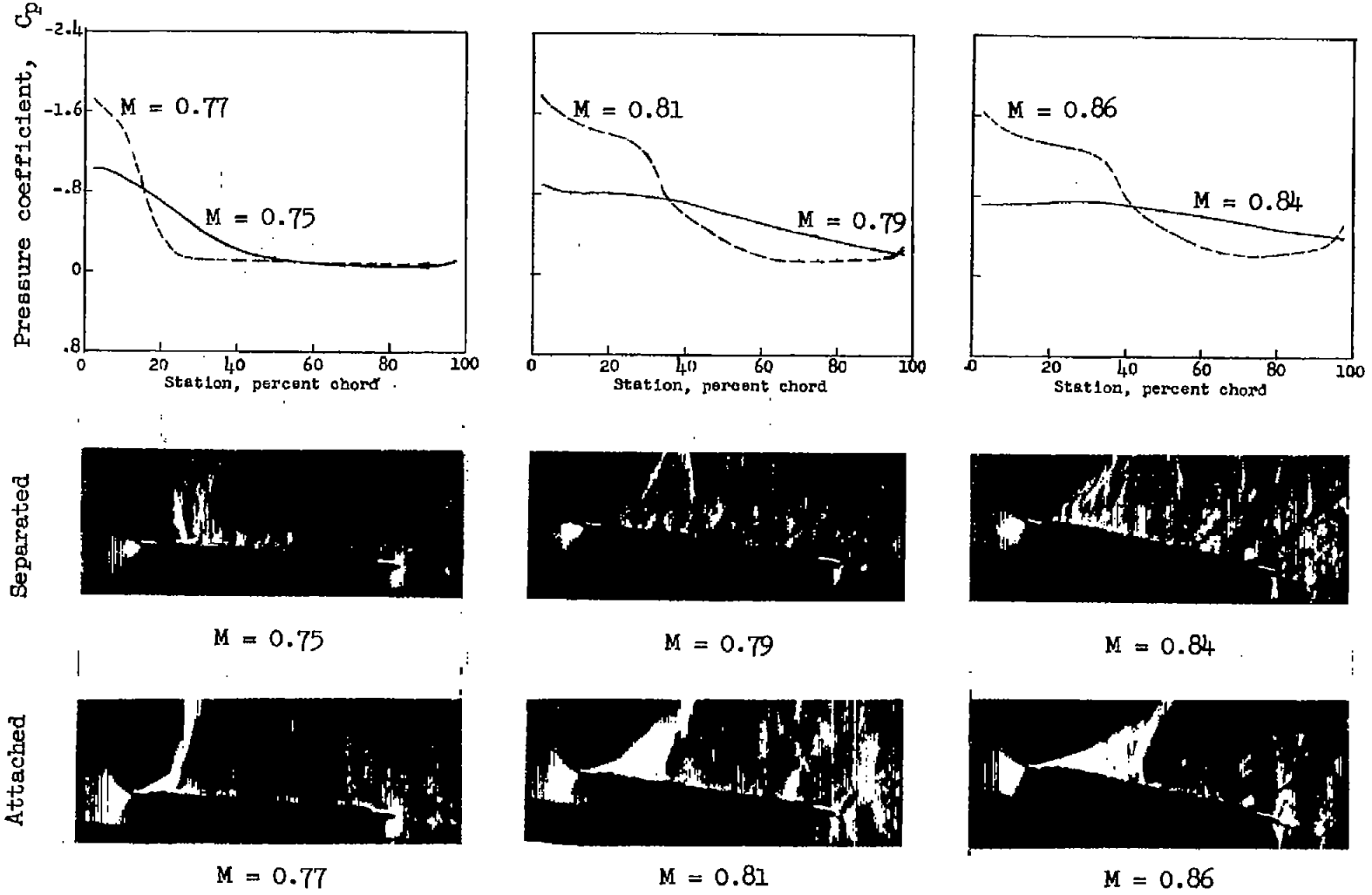

(a) $\alpha = 4^\circ$. (b) $\alpha = 8^\circ$. (c) $\alpha = 10^\circ$.

L-86434

Figure 15.- Flow past a slab airfoil having a 1:1 elliptically shaped leading edge.

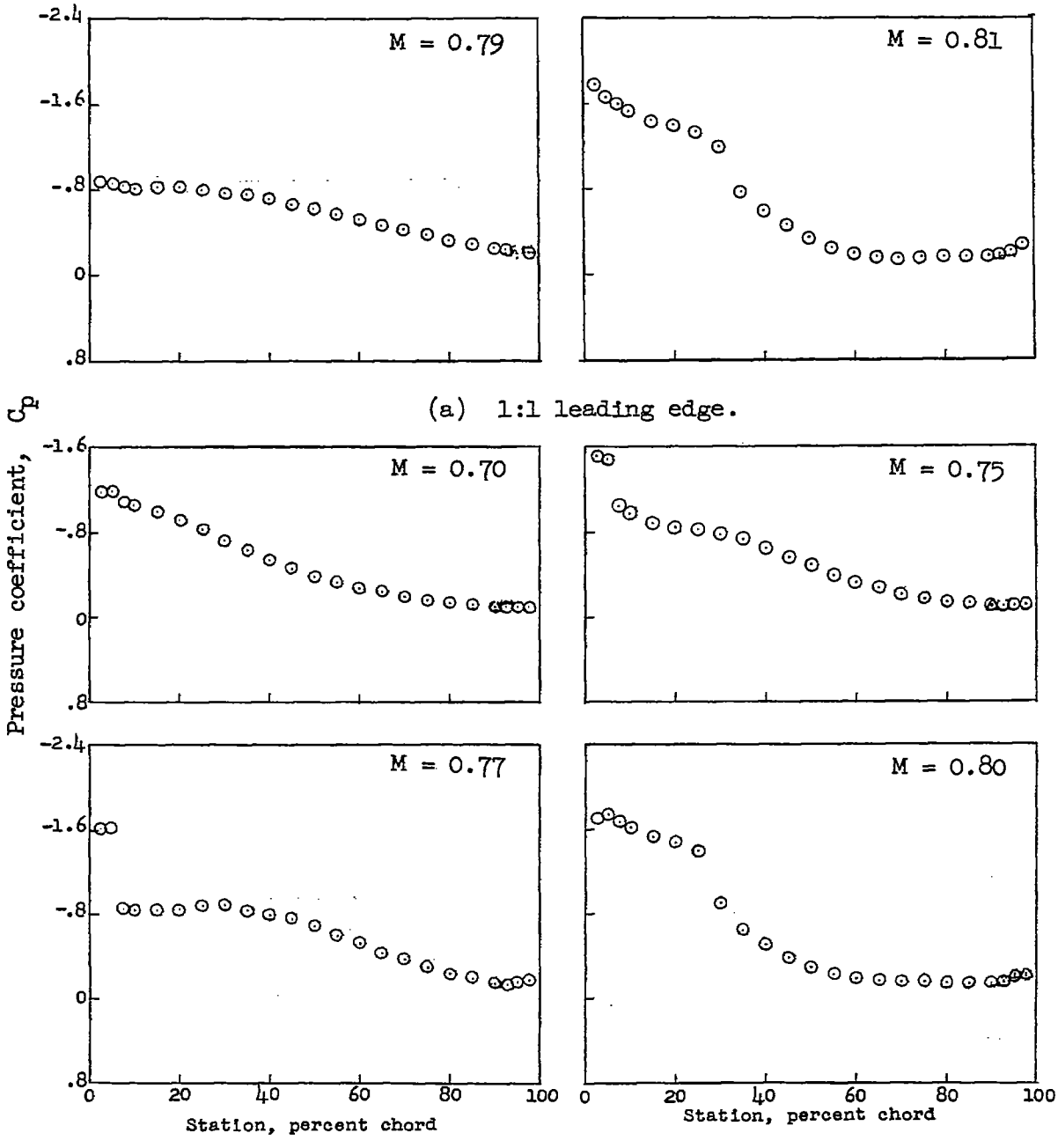

(b) 4:1 leading edge.

Figure 16.- Effects of leading-edge shape of slab airfoil on pressures at transonic-flow attachment. $\alpha = 8^{\circ}$.

M = 0.79

M = 0.80

(a) 1:1 leading edge.

M = 0.70

M = 0.75

M = 0.77

M = 0.80

(b) 4:1 leading edge.

L-86435

Figure 17.- Effects of leading-edge shape of slab airfoil on flow at transonic-flow attachment. $\alpha = 8^{\circ}$.

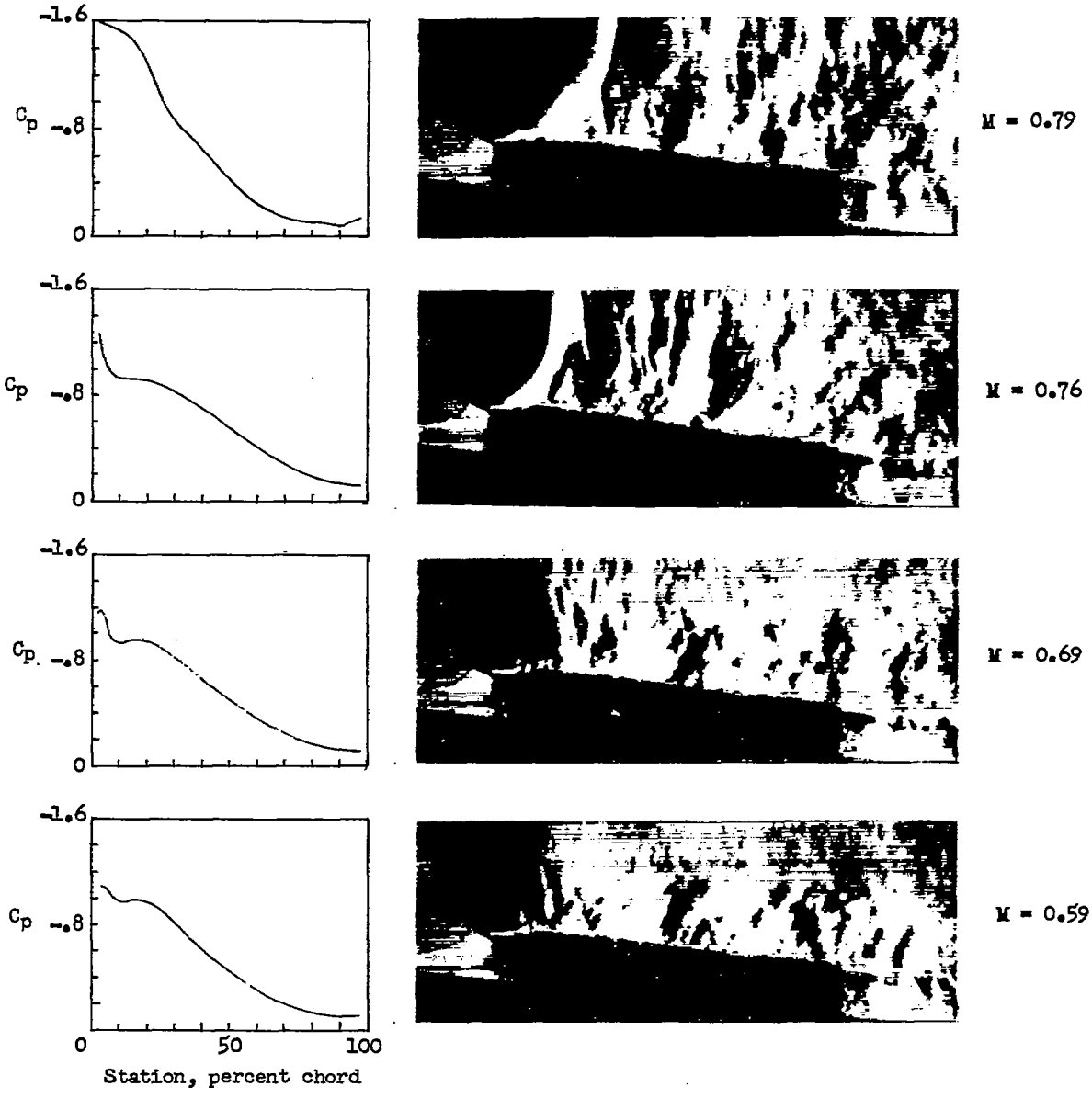

L-57-4446

Figure 18.- Flow past a slab airfoil having a 10:1 leading edge illustrating gradual flow attachment. $\alpha = 8^{\circ}$.

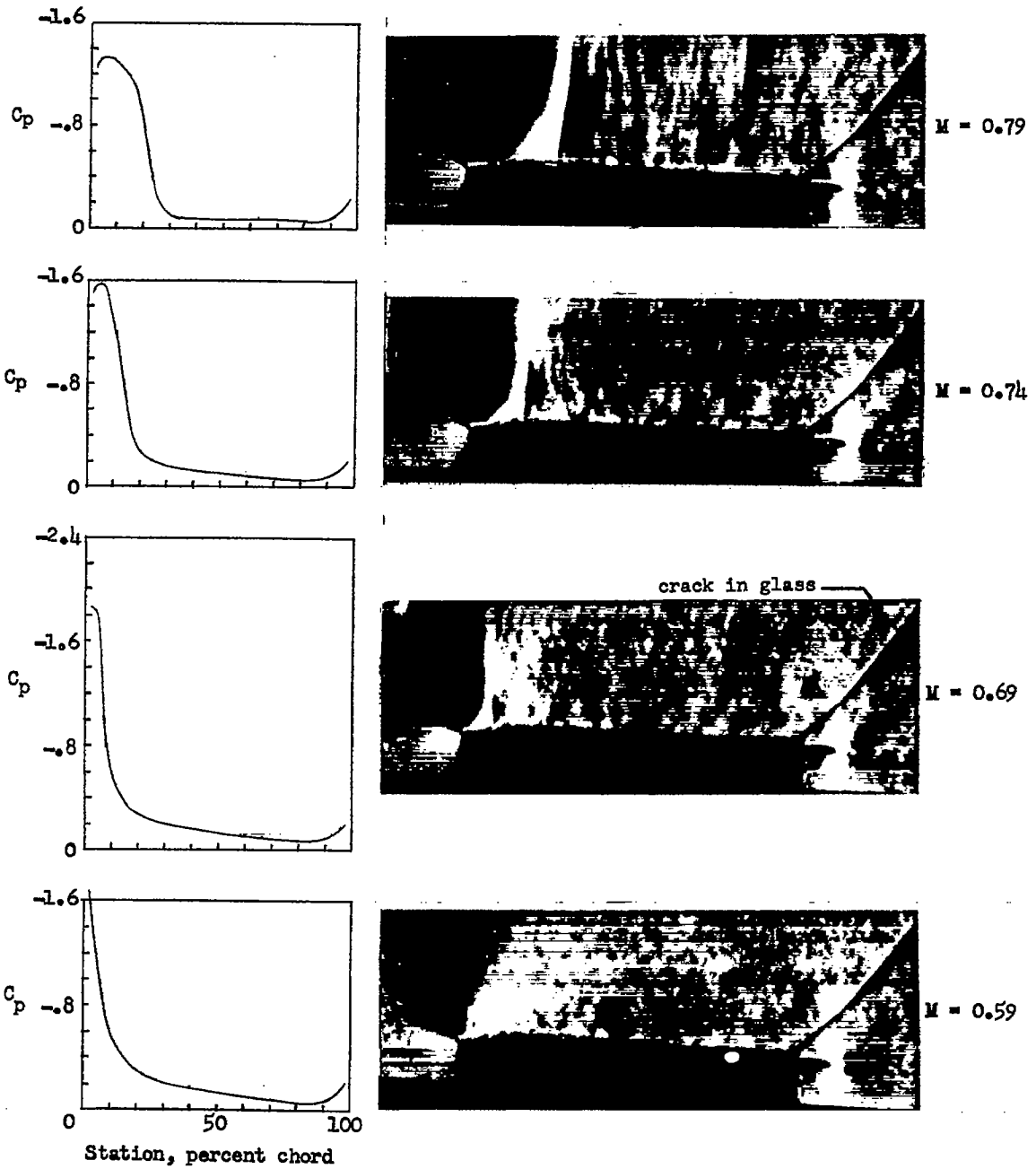

L-57-4447

Figure 19.- Flow past a slab airfoil having a 10:1 leading edge. $\alpha = 4^\circ$.

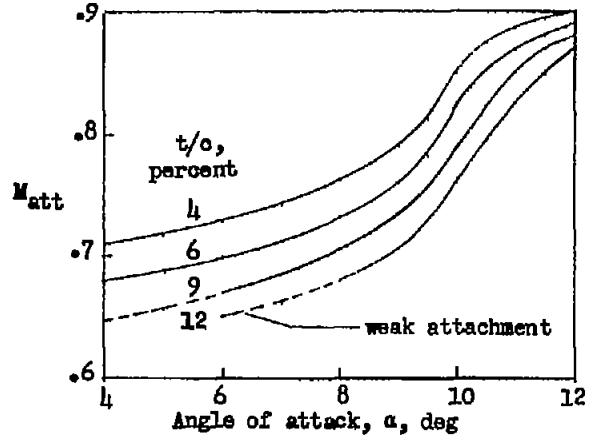

(a) NACA 64AOXX airfoils.

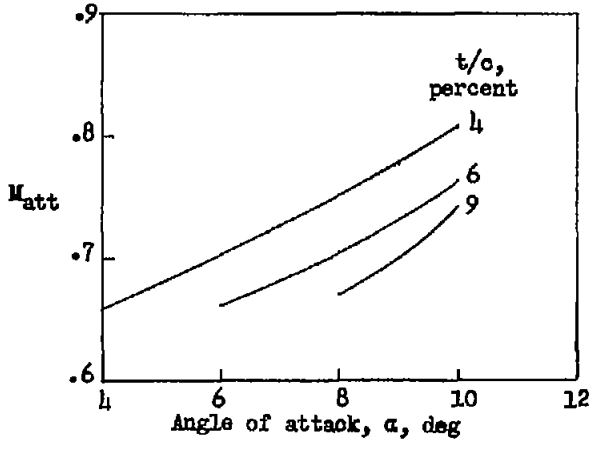

(b) NACA 65AOXX airfoils.

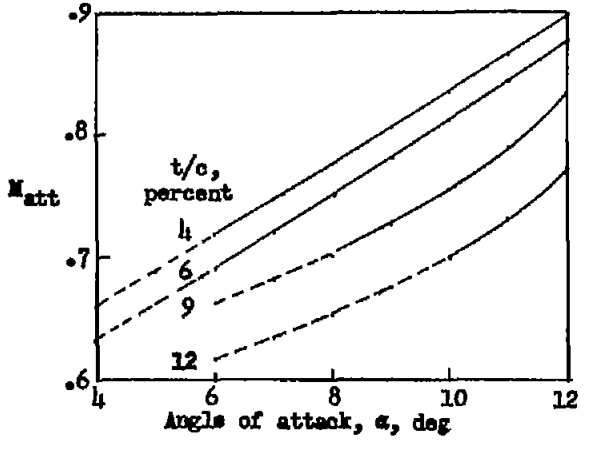

(c) NACA 16-OXX airfoils.

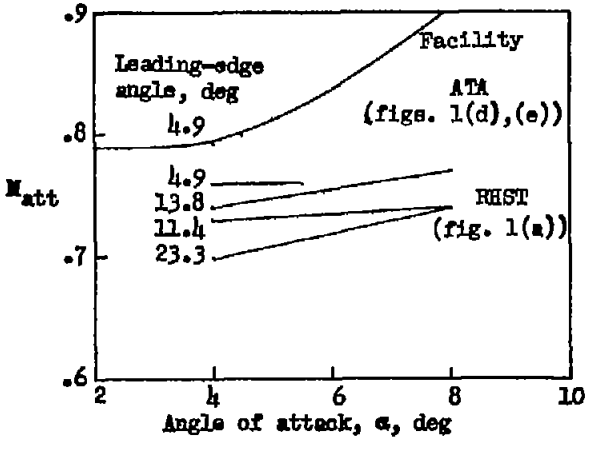

(d) Supersonic-type airfoils.

Figure 20.- Mach number for flow attachment on airfoils as affected by angle of attack.

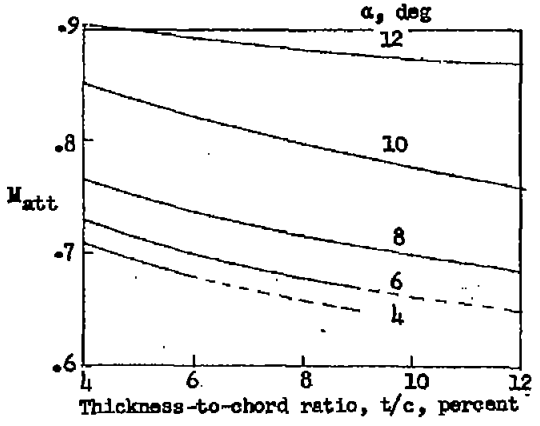

(a) NACA 64A0XX airfoils.

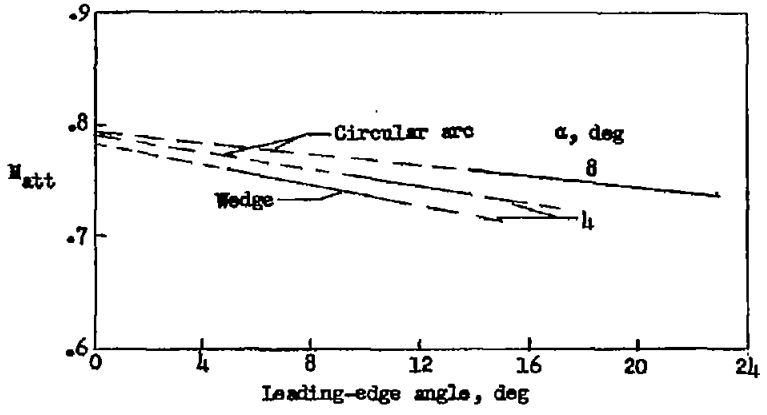

(b) Supersonic-type airfoils.

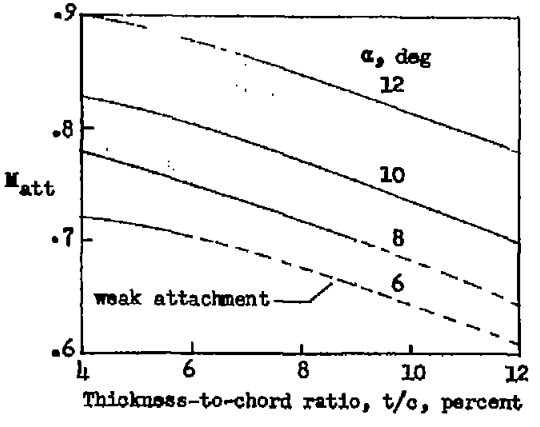

(c) NACA 16-0XX airfoils.

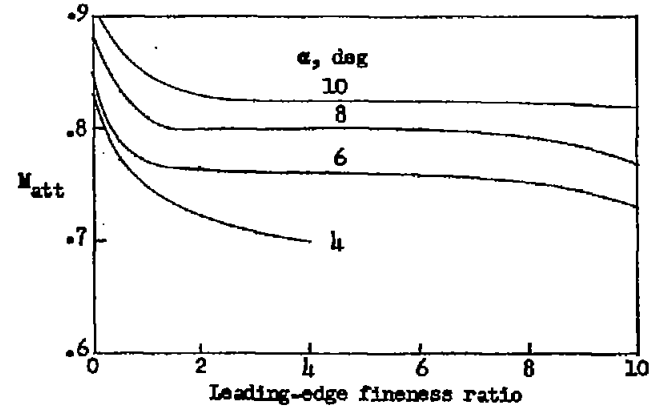

(d) Slab airfoils.

Figure 21.- Mach number for flow attachment on airfoils as affected by thickness and leading-edge shape.

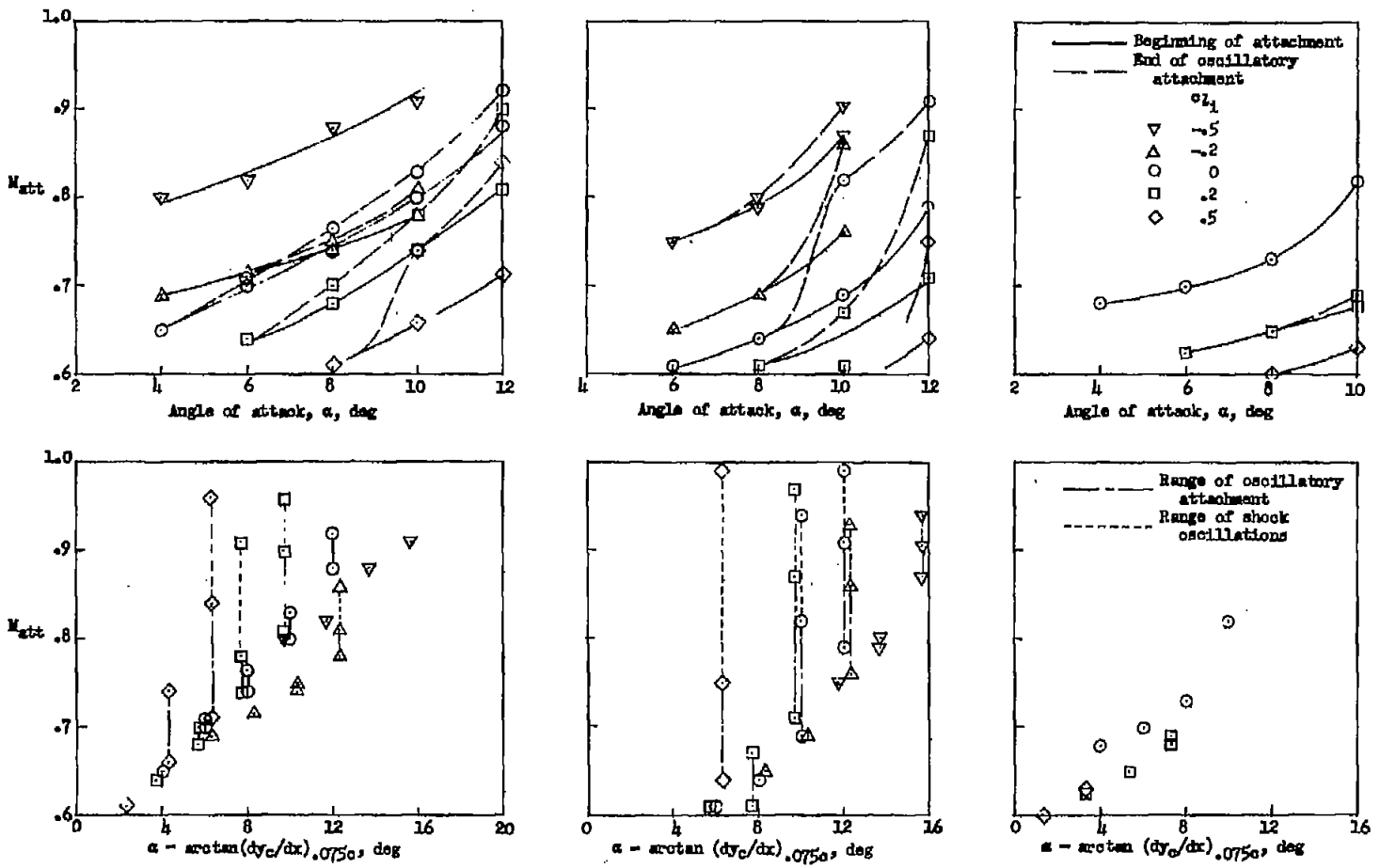

(a) NACA 16-X06 airfoils. (b) NACA 16-X12 airfoils. (c) NACA 64AX06 airfoils.

Figure 22.- Effects of camber on transonic-flow attachment.

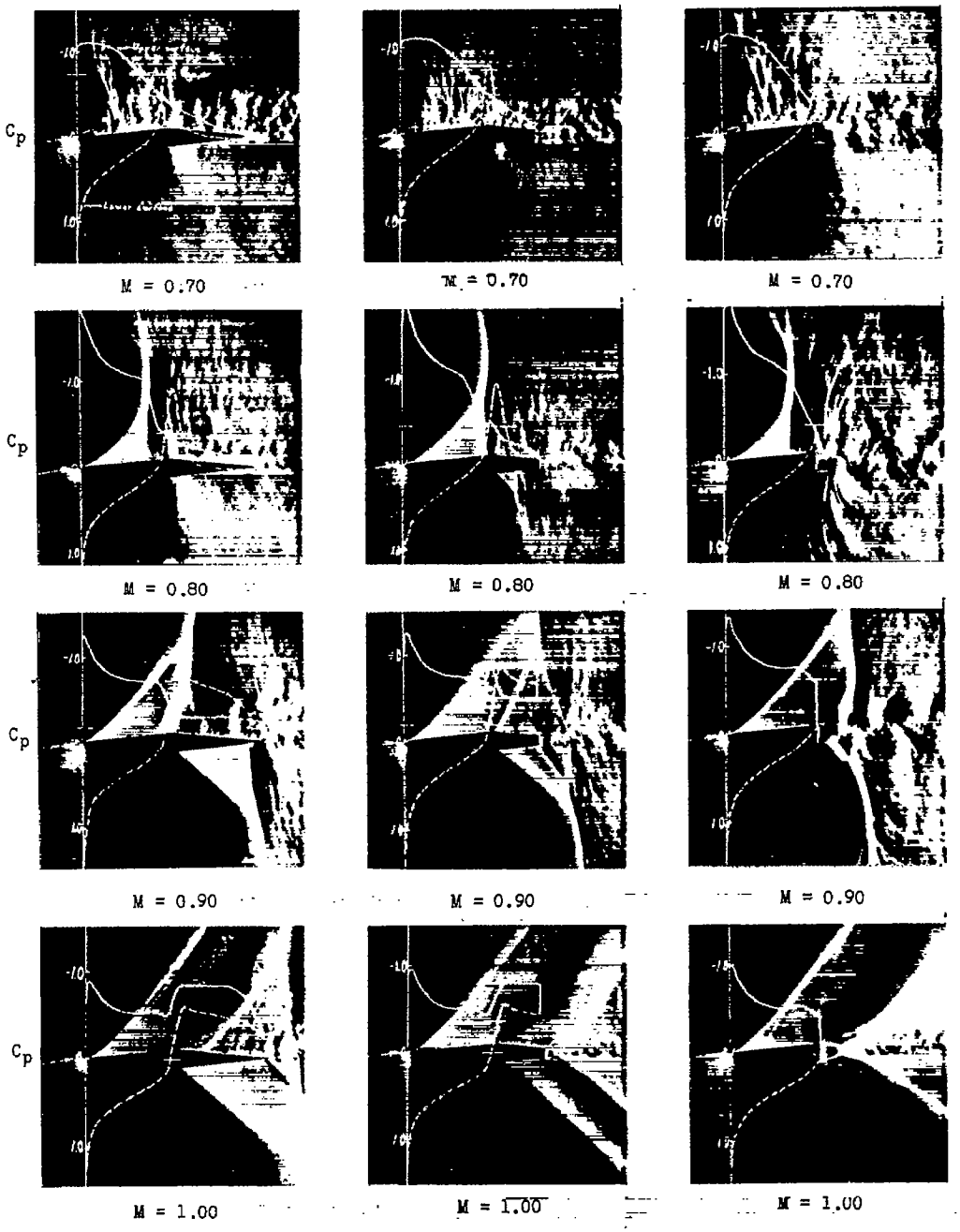

(a) Basic model. (10-W-5)

(b) Basic model cut off at 0.75 chord. (13-W-6.6)

(c) Basic model cut off at 0.50 chord. (20-W-10)

L-57-4448

Figure 23.- Effect of afterbody on flow over a wedge-shaped forebody. $\alpha = 8^{\circ}$.

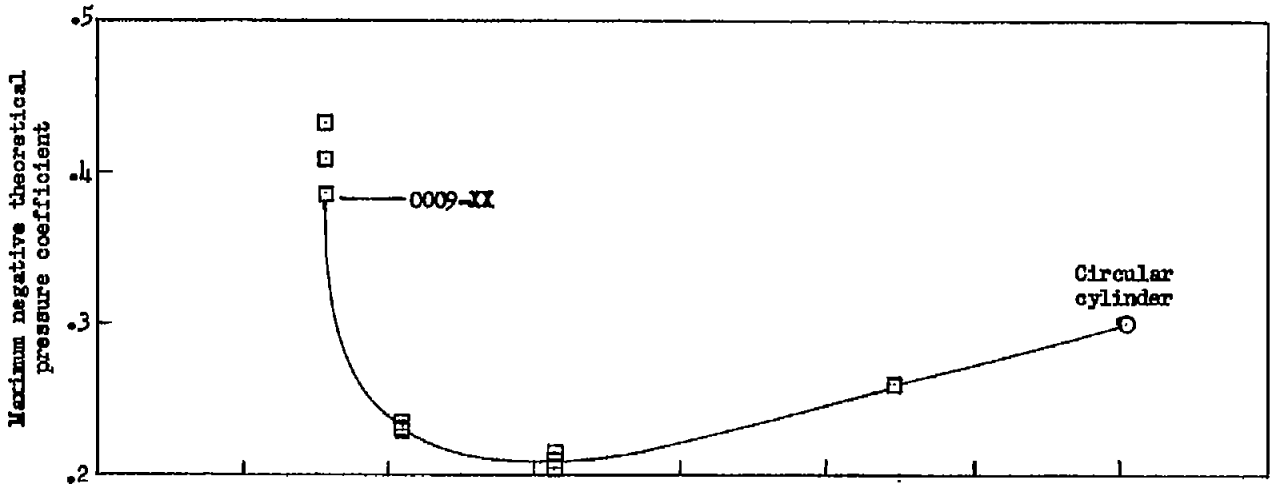

(a) Maximum negative theoretical pressure coefficient. $c_n = 0.5$.

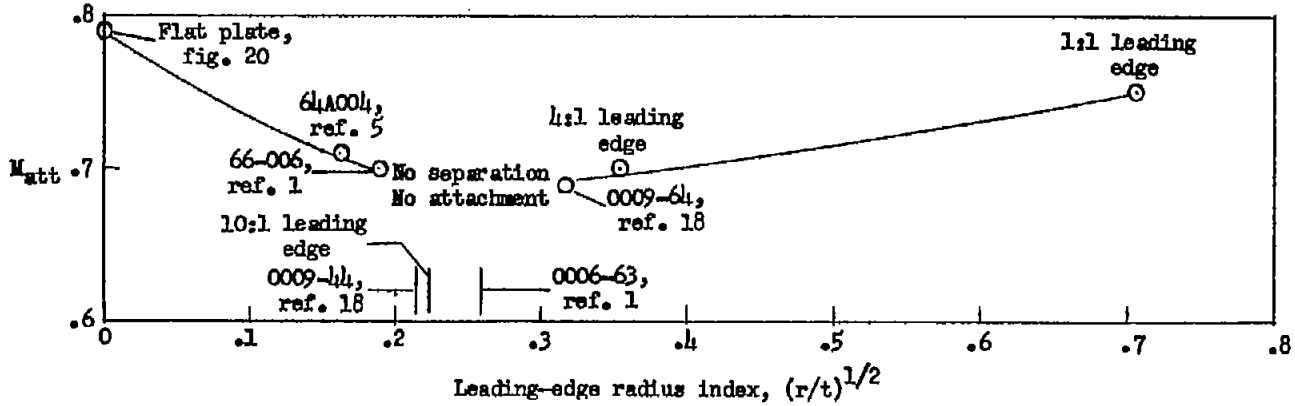

(b) Mach number for transonic-flow attachment.

Figure 24.- Correlation of leading-edge-shape effects on transonic-flow attachment. $\alpha = 4^{\circ}$.

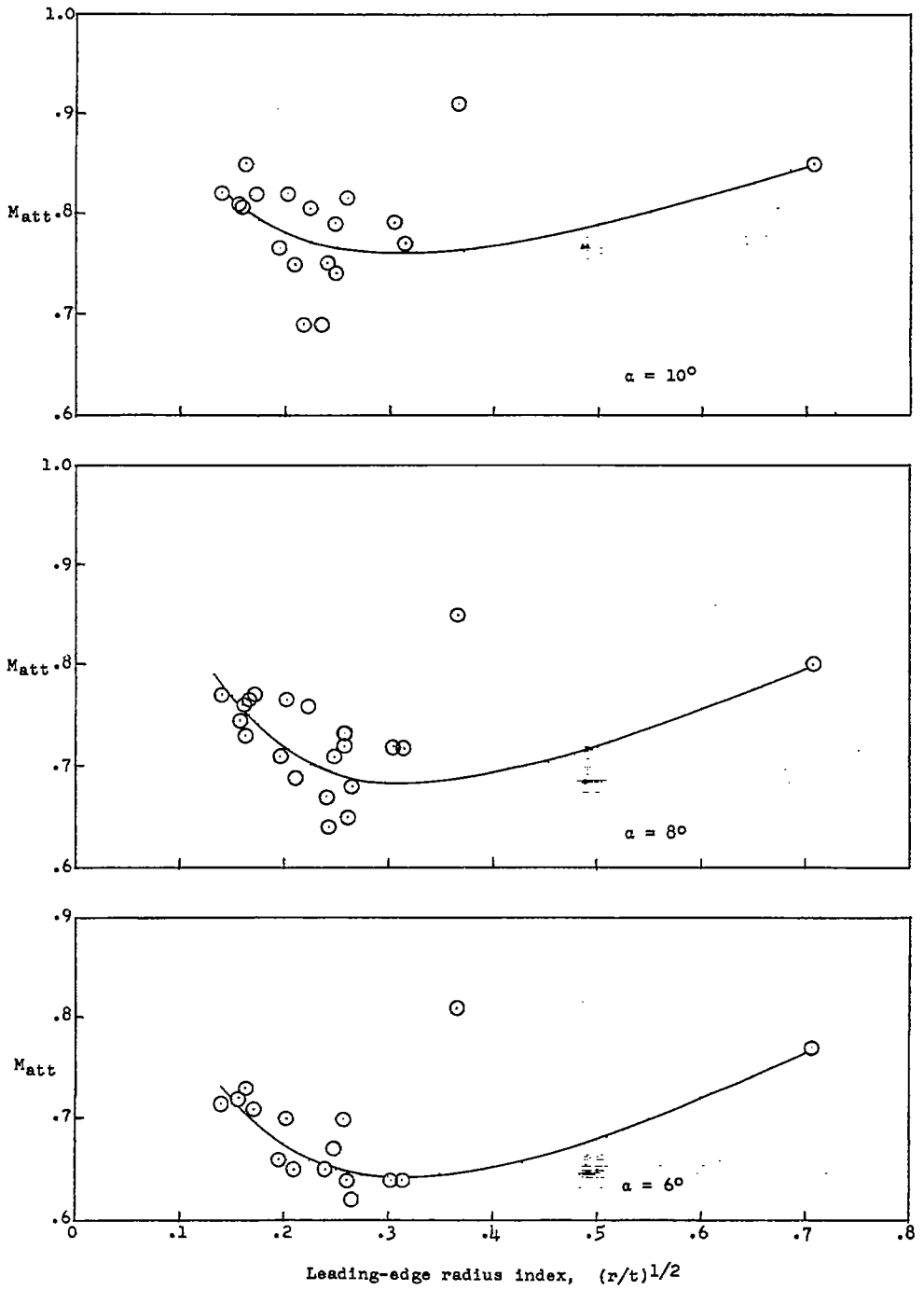

Figure 25.- Mach number for attachment as affected by leading-edge-radius index at several angles of attack.

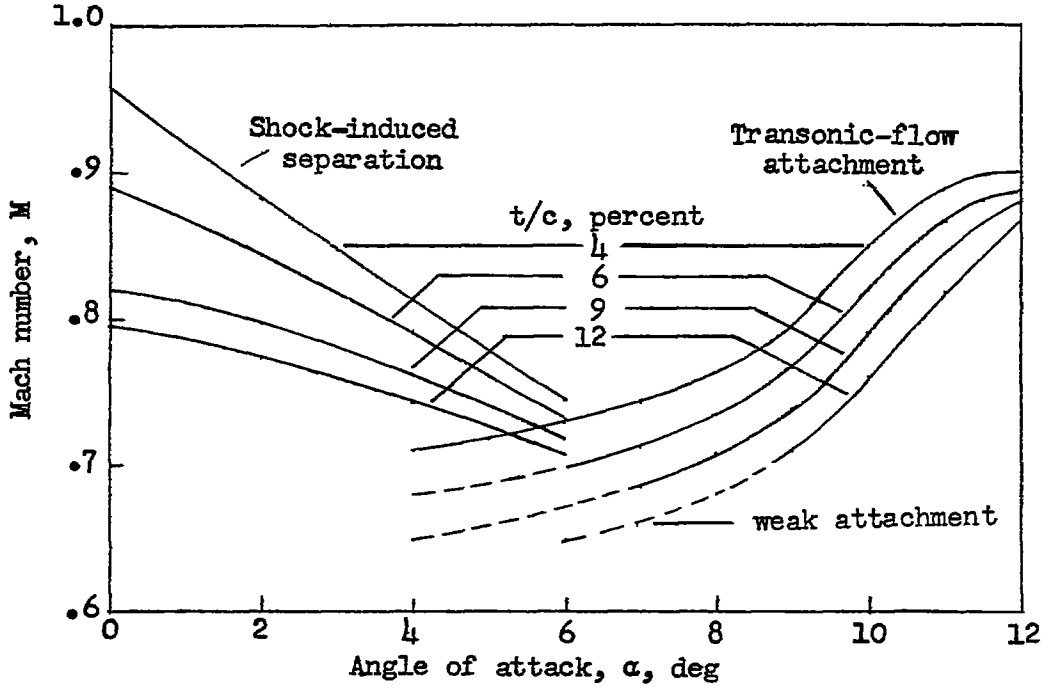

Figure 26.- Boundaries for transonic-flow attachment and shock-induced separation on NACA 64AOXX airfoils.

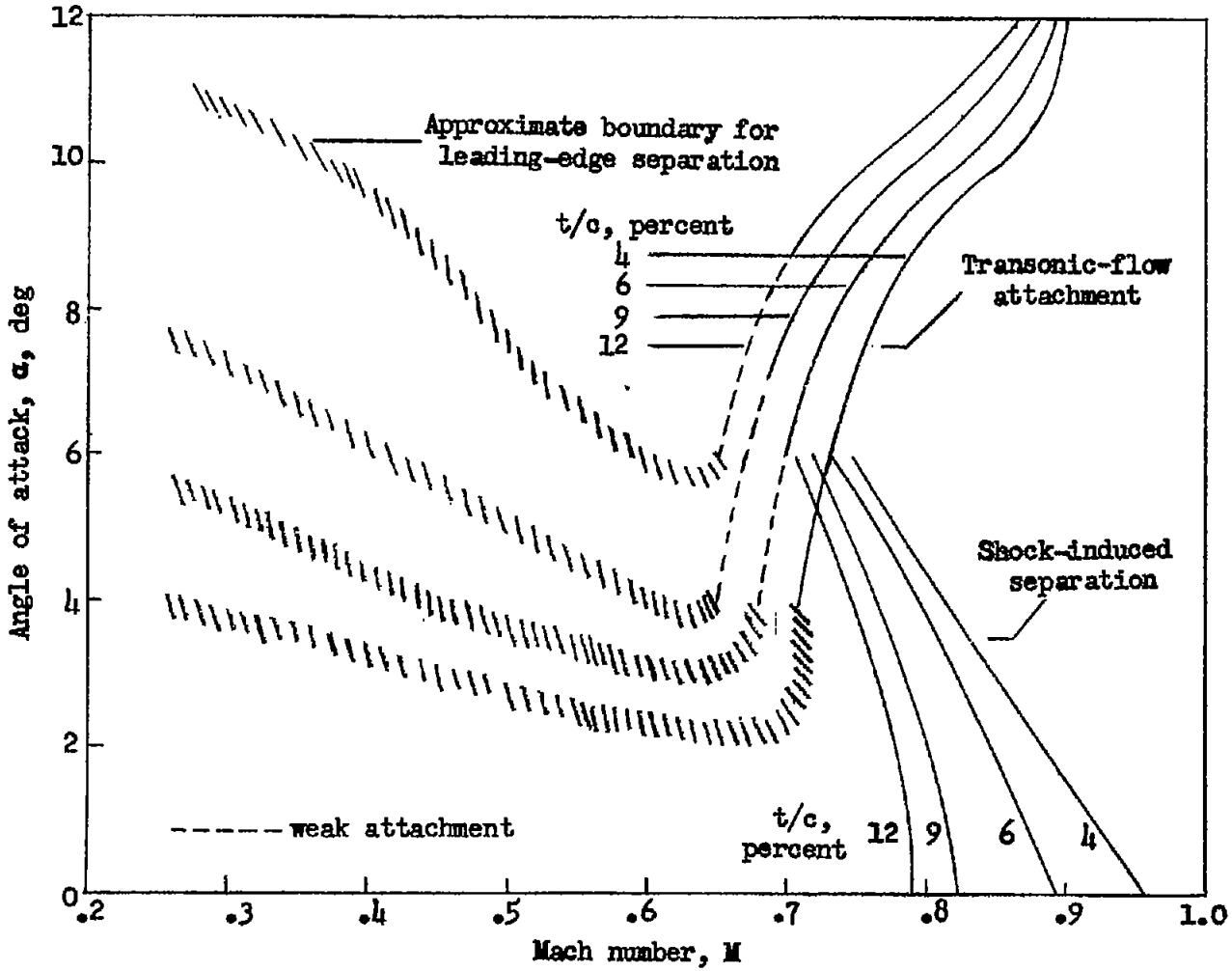

Figure 27.- Boundaries of angle of attack against Mach number for flow separation and attachment.

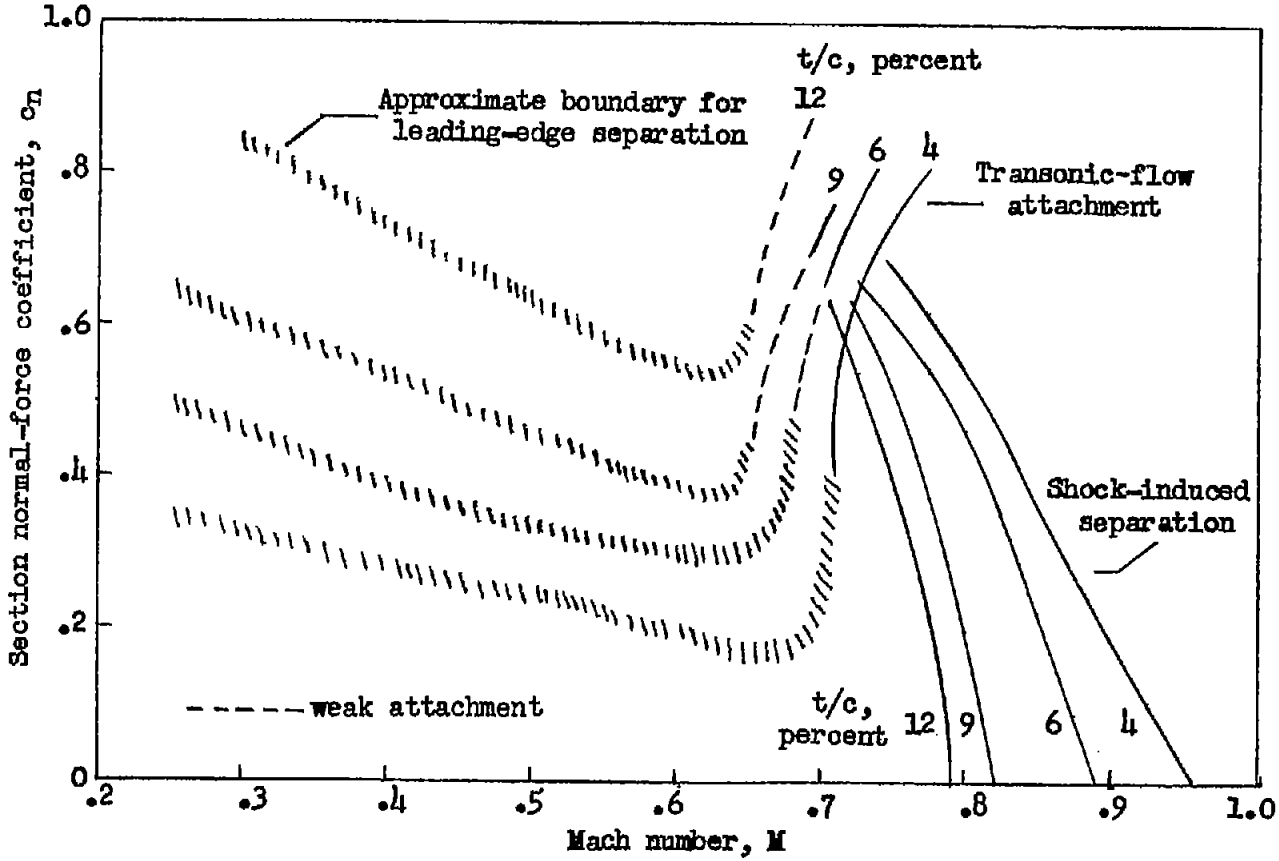

Figure 28.- Boundaries of normal force against Mach number for flow separation and attachment.

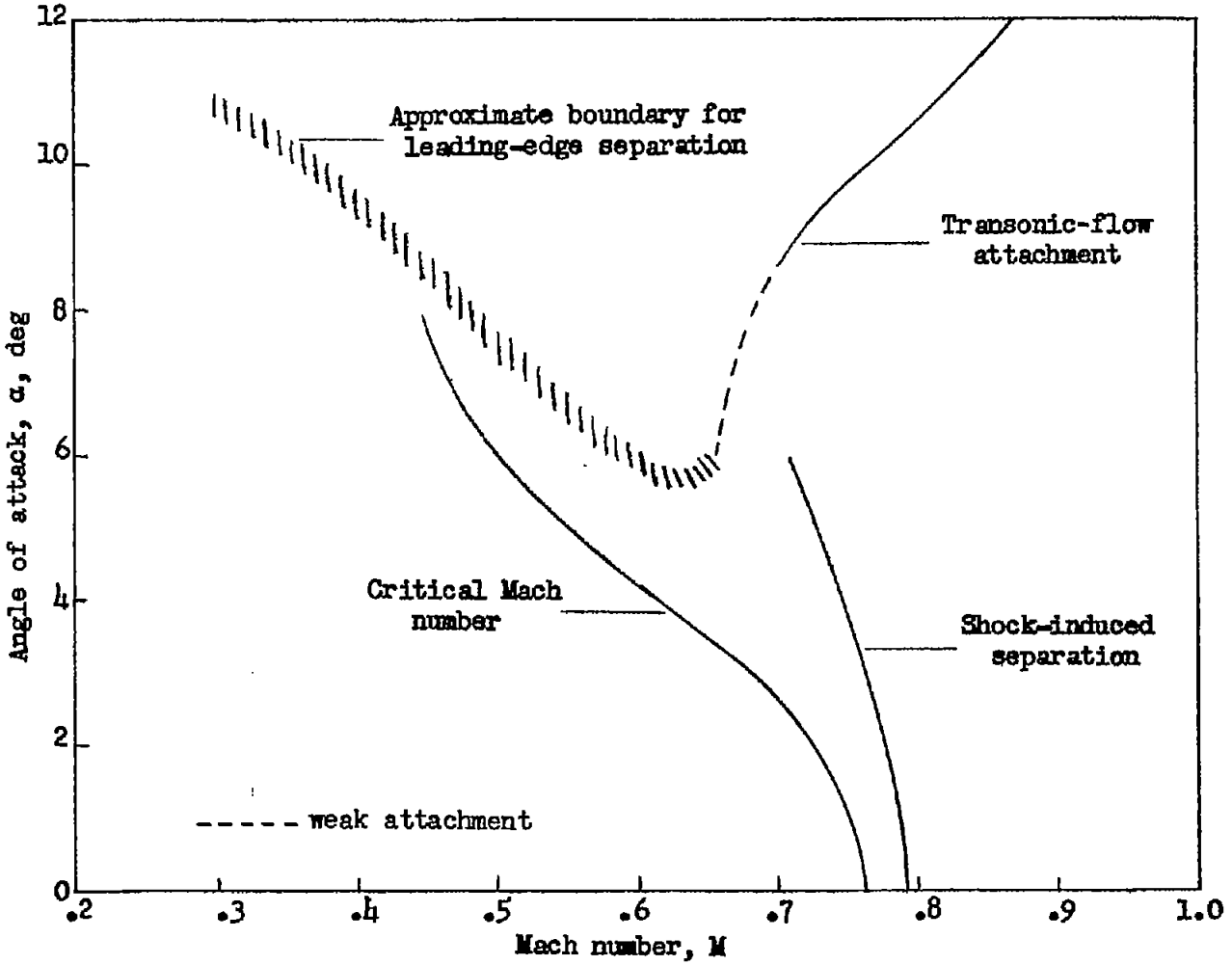

(a) NACA 64A012 airfoil.

Figure 29.- Flow boundaries for NACA 64A-series airfoils.

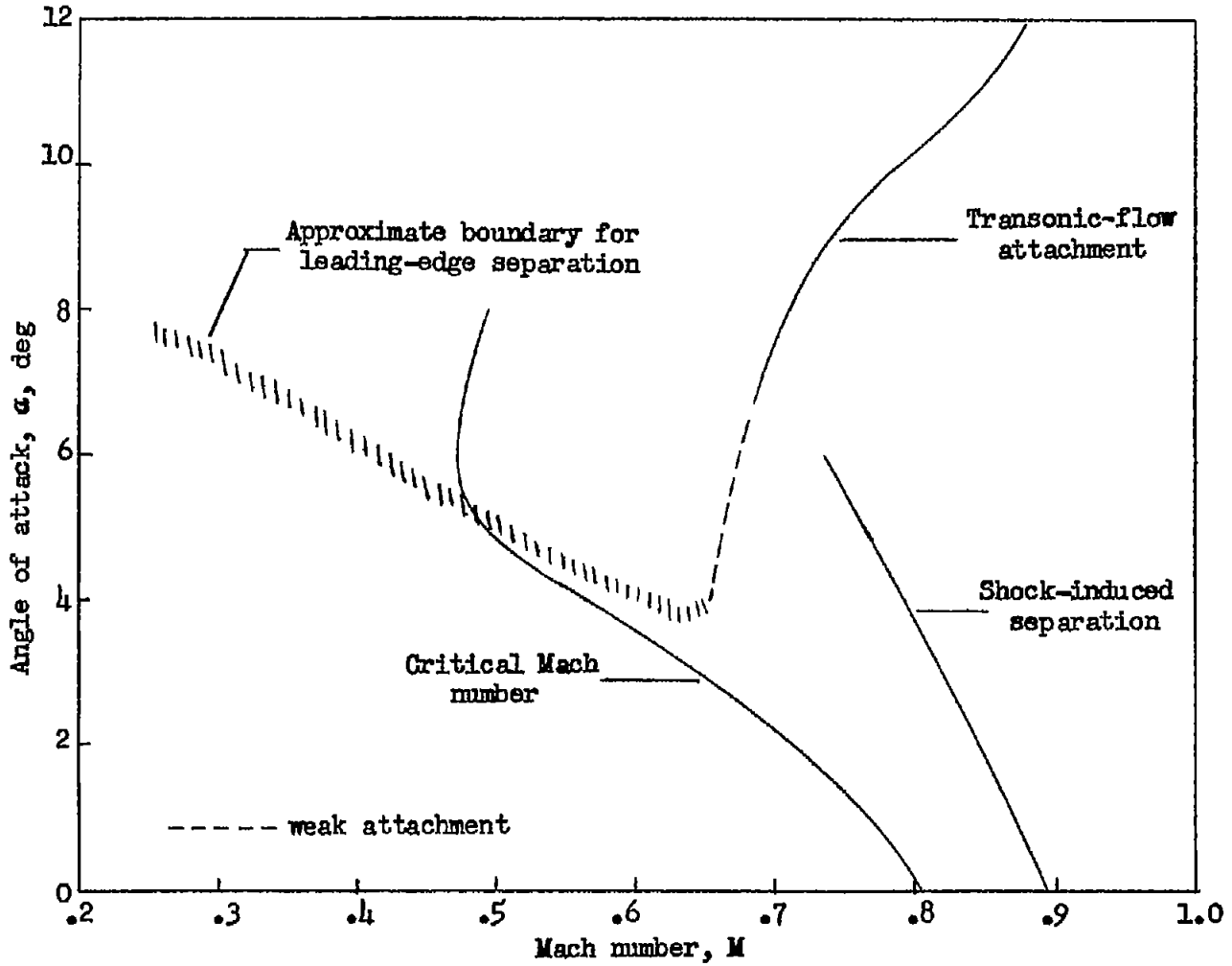

(b) NACA 64A009 airfoil.

Figure 29.- Continued.

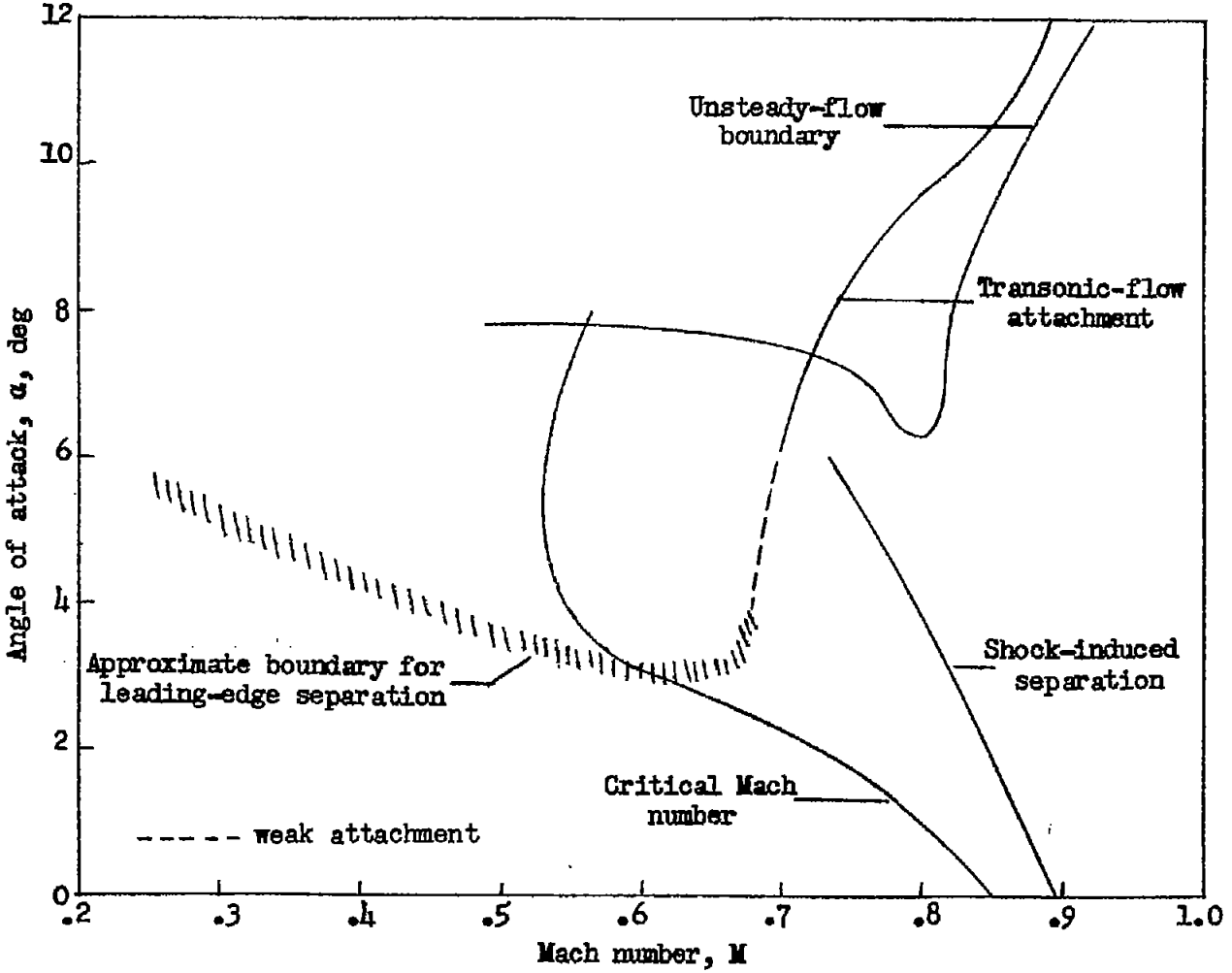

(c) NACA 64A006 airfoil.

Figure 29.- Continued.

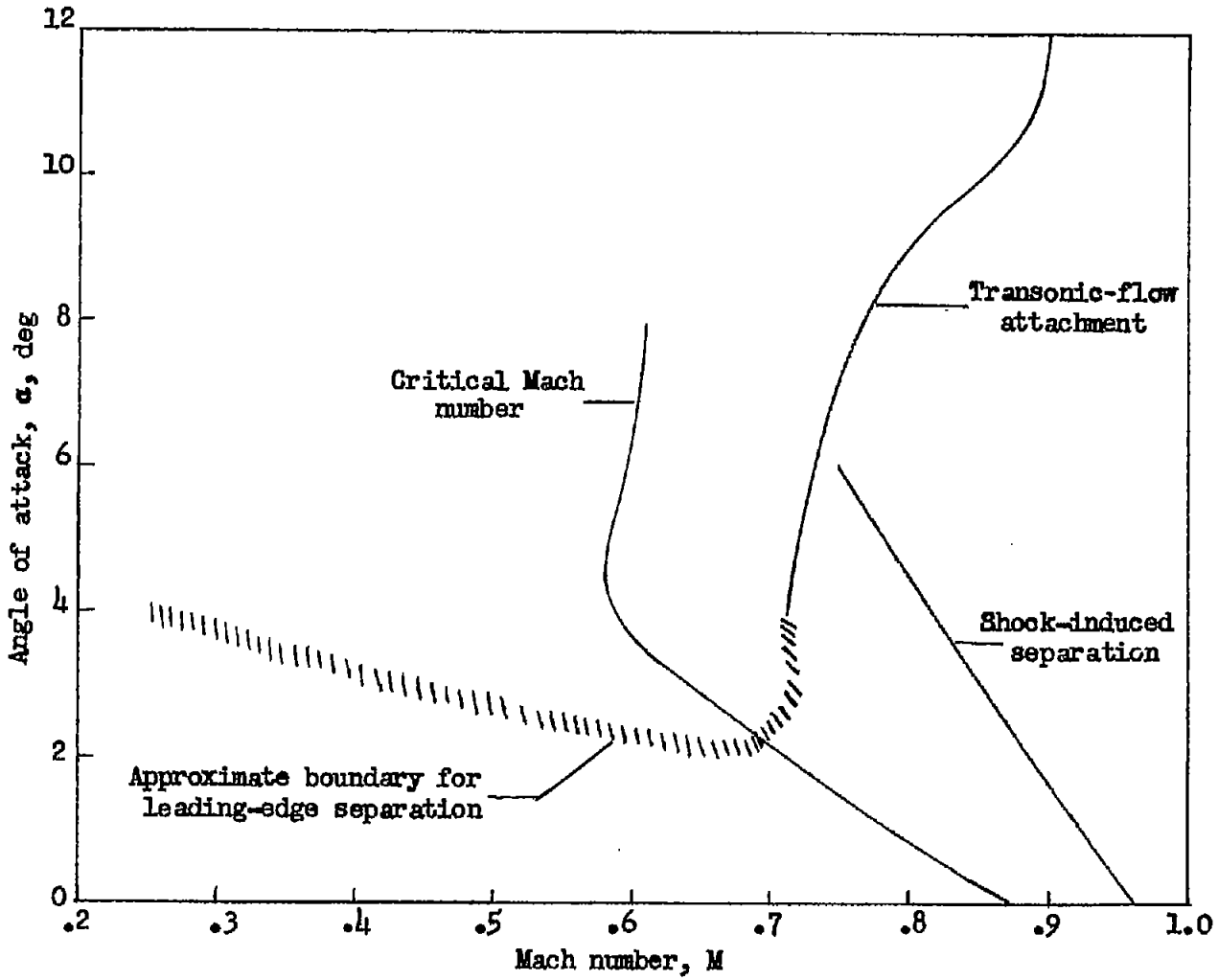

(d) NACA 64A004 airfoil.

Figure 29.- Concluded.

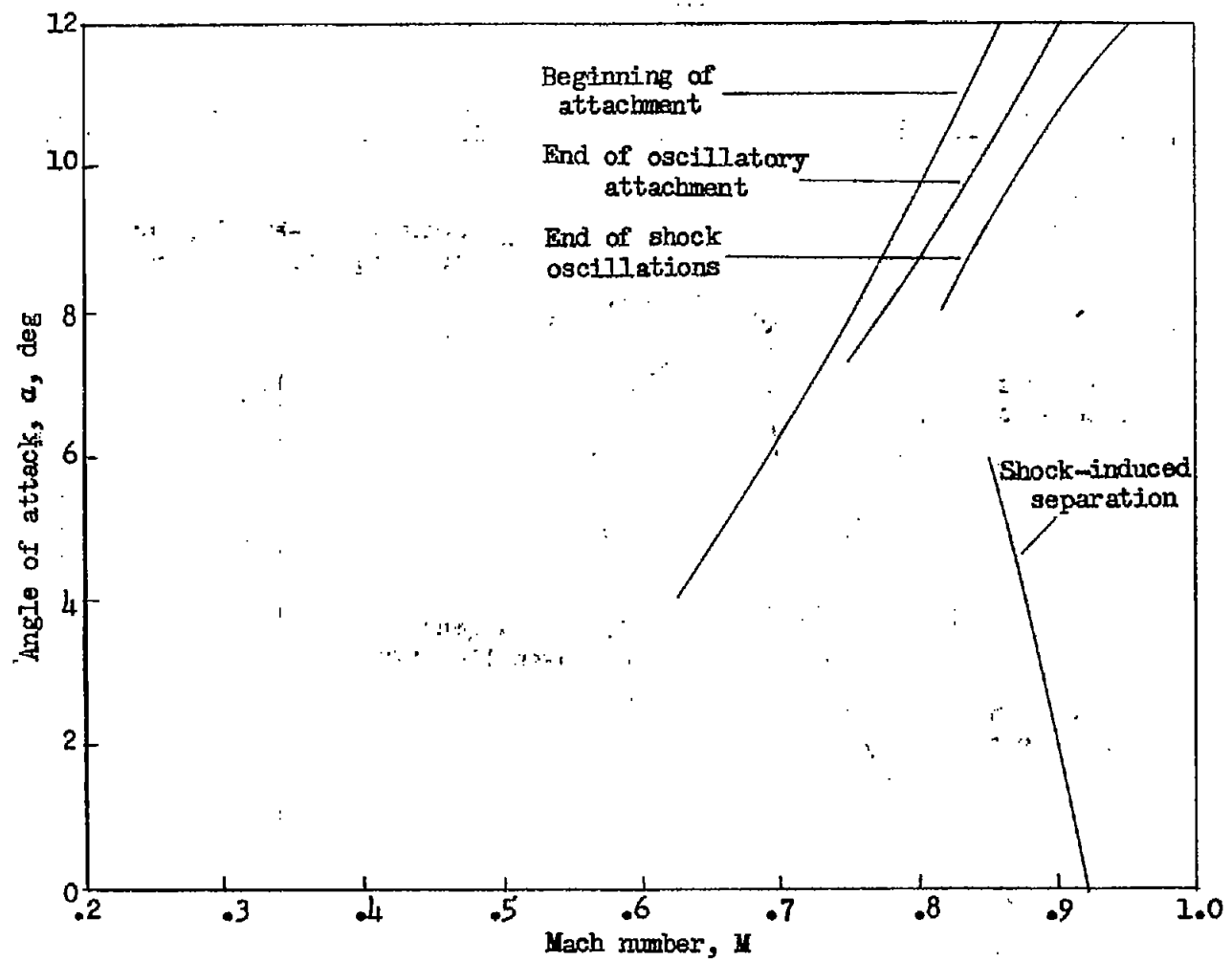

Figure 30.- Flow boundaries for an NACA 16-006 airfoil.

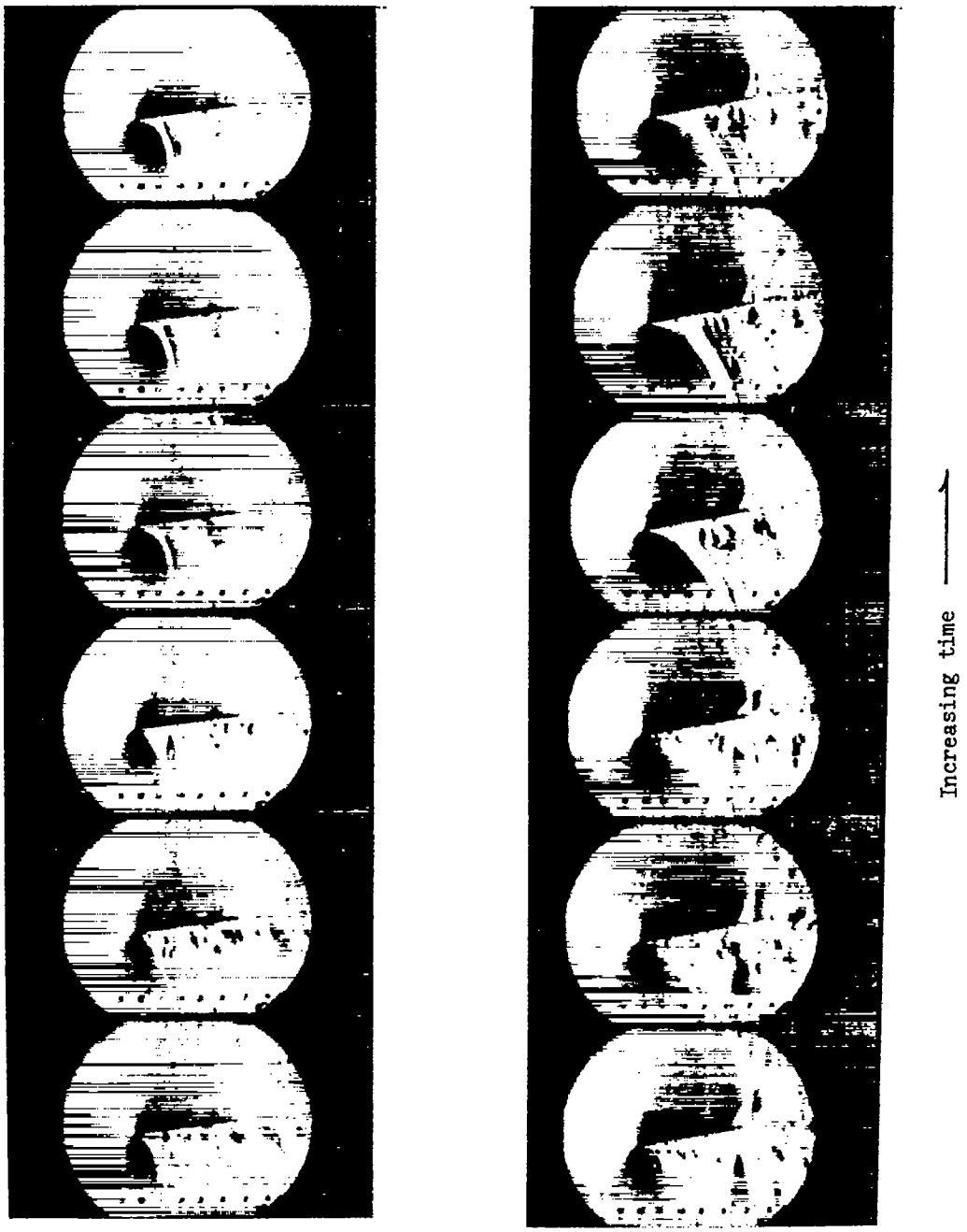

$\alpha = -6°$
$M \approx 0.84$

$\alpha = -10°$
$M \approx 0.91$

L-57-4449

Figure 31.- Abrupt attachment. NACA 16-506 airfoil.

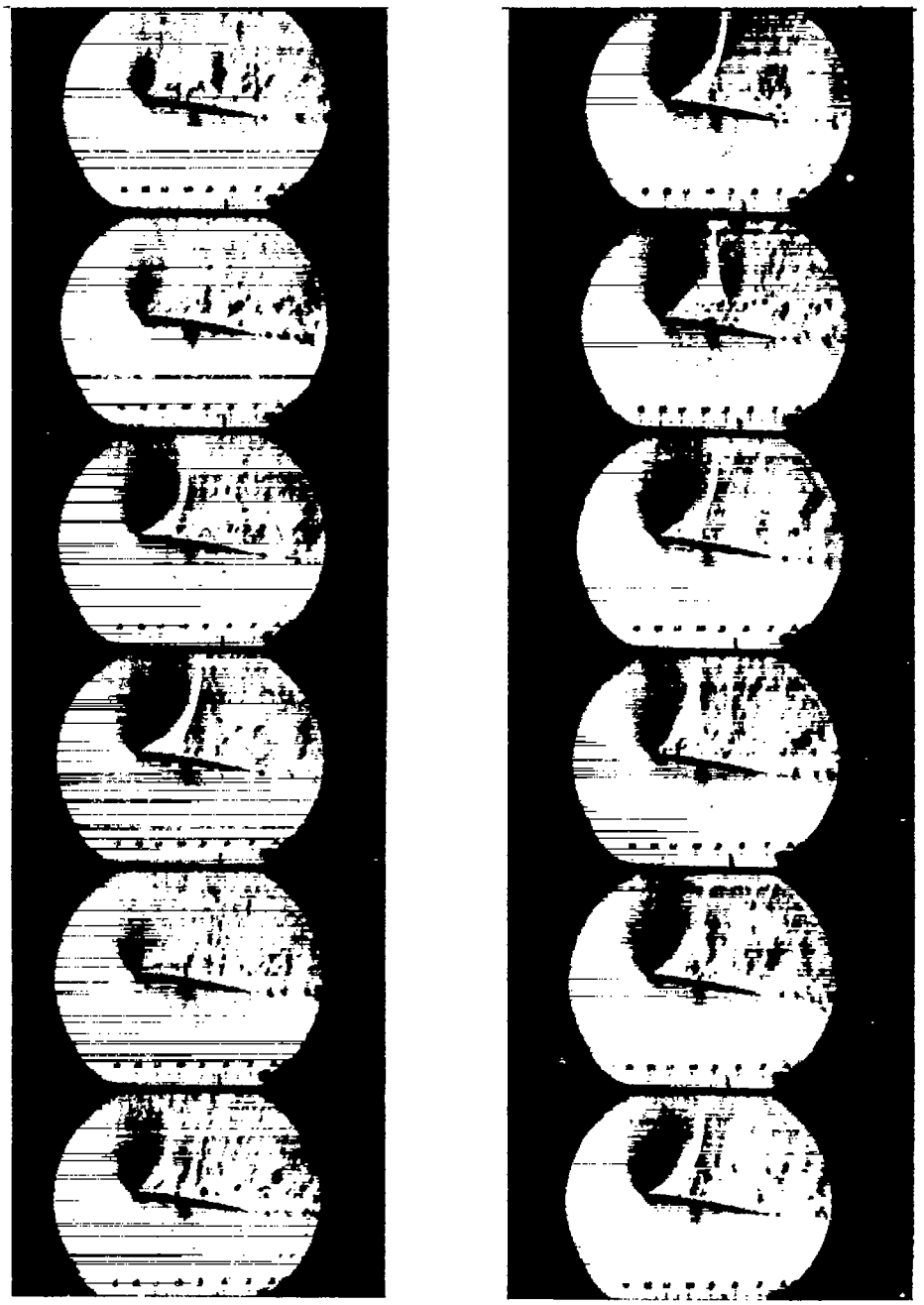

Beginning of oscillations
$M \approx 0.825$

Near end of oscillations
$M \approx 0.845$

L-57-4450

Figure 32.- Oscillatory attachment. NACA 16-006 airfoil; $\alpha = 10^{\circ}$.

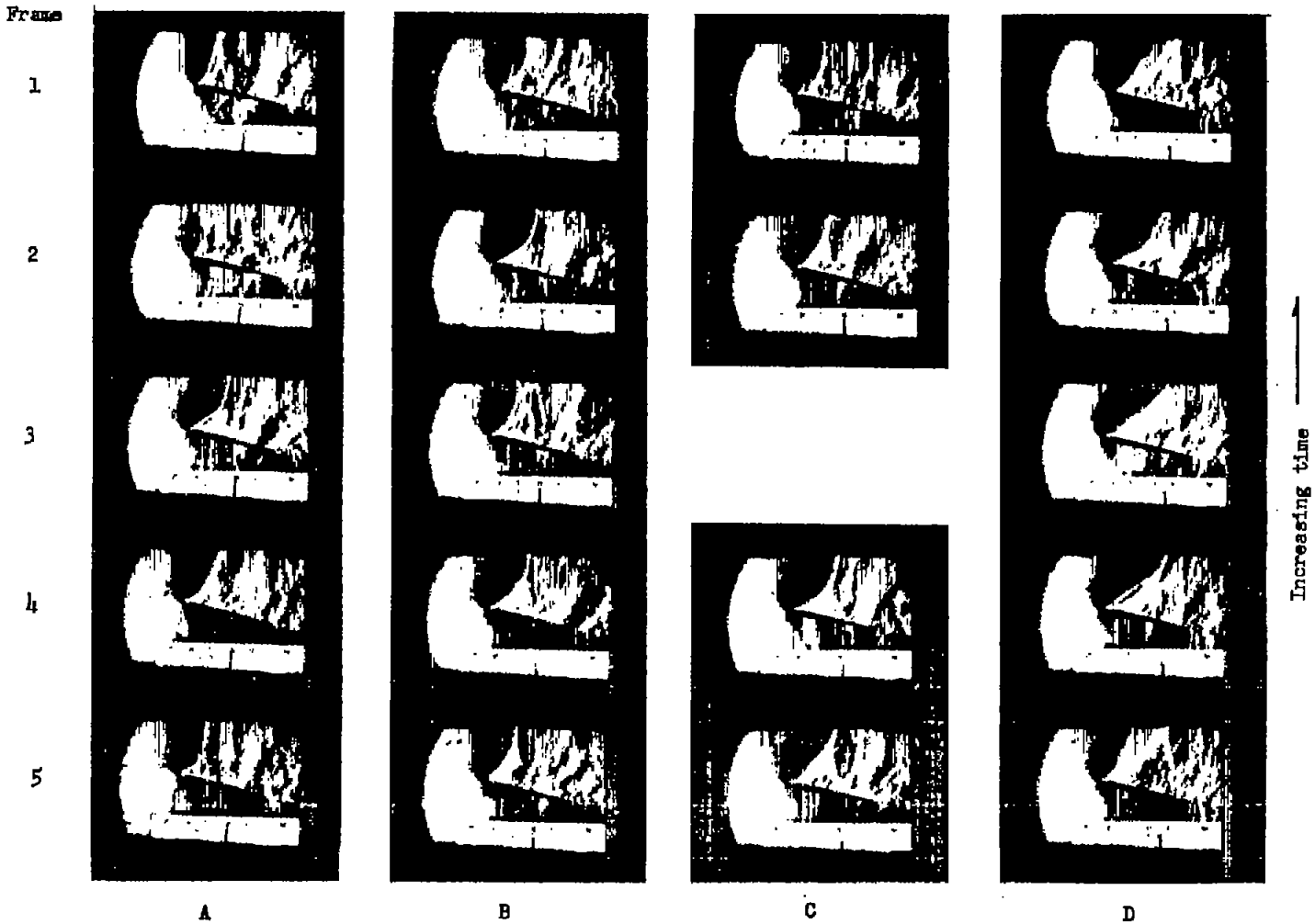

L-57-4451

ure 33.- Development of oscillatory attachment. Film speed, approximately 300 frames per second; NACA 4-006 airfoil; $\alpha = 10^{\circ}$.

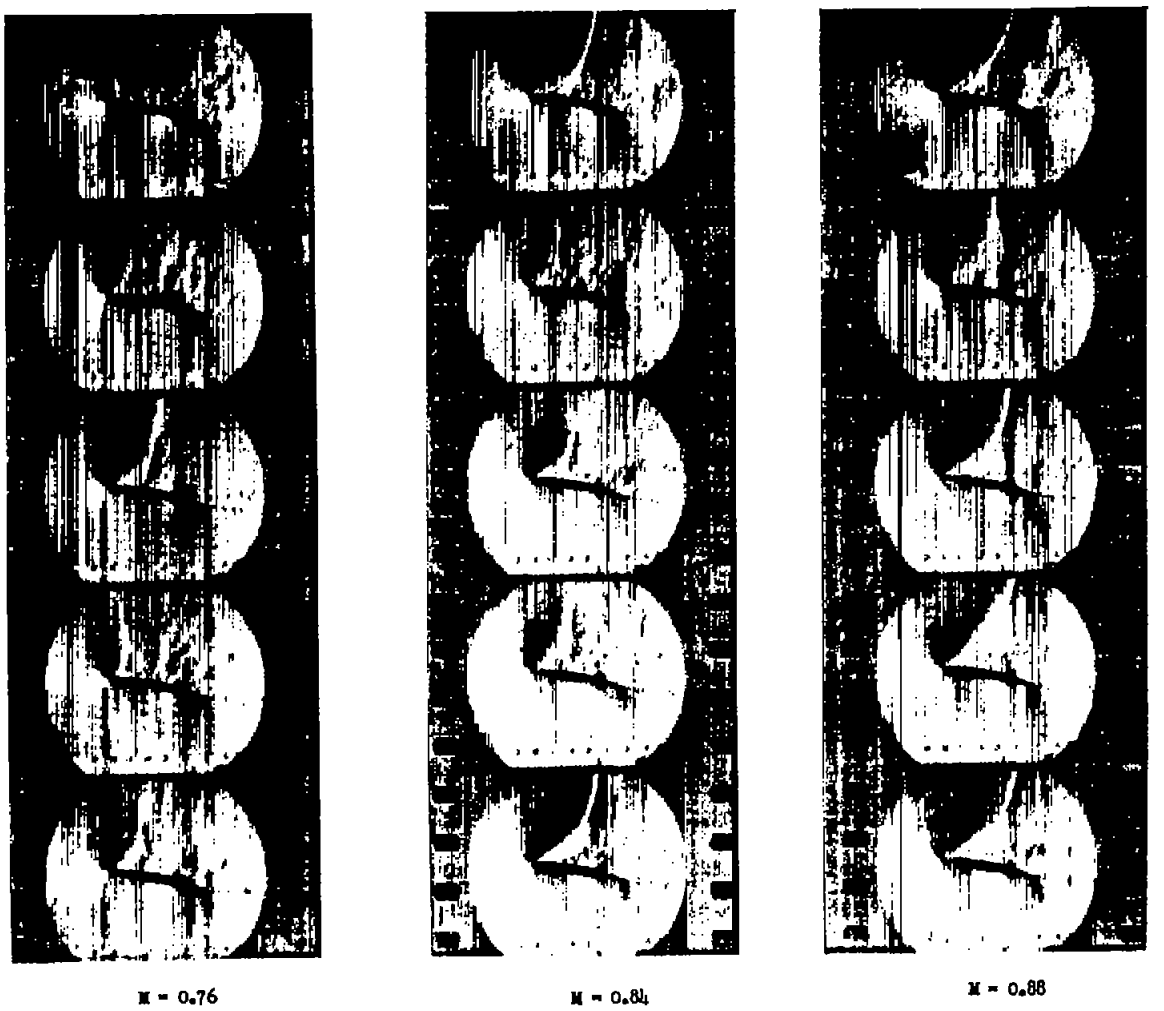

L-57-4452

Figure 34.- Oscillatory attachment. NACA 64A009 airfoil with a 30-percent trailing-edge flap deflected 8°; $\alpha = 10°$.

(a) Smooth model.

(b) Transition fixed at front edge.

Figure 35.- Flow past a cylindrical-shaped body of revolution. L-57-4453